Turkish Journal of Mathematics

Volume 45 | Number 6 Article 6

1-1-2021

On the distribution of coefficients of half-integral weight modular forms and the Bruinier-Kohnen Conjecture

İLKER İNAM

ZEYNEP DEMİRKOL ÖZKAYA

ELİF TERCAN

GABOR WIESE

TÜBİTAK

Turkish Journal of Mathematics

http://journals.tubitak.gov.tr/math/

Research Article

Turk J Math
(2021) 45: 2427 – 2440
© TÜBİTAK
doi:10.3906/mat-2105-40

On the distribution of coefficients of half-integral weight modular forms and the Bruinier–Kohnen conjecture

İlker İNAM[1,*], Zeynep DEMİRKOL ÖZKAYA[2], Elif TERCAN[1], Gabor WIESE[3]

[1]Department of Mathematics, Faculty of Arts and Sciences, Bilecik Şeyh Edebali University, Bilecik, Turkey
[2]Muradiye Vocational School, Van Yüzüncüyıl University, Van, Turkey
[3]Department of Mathematics, University of Luxembourg, Esch-sur-Alzette, Luxembourg

Received: 13.05.2021 • **Accepted/Published Online:** 23.08.2021 • **Final Version:** 29.11.2021

Abstract: This work represents a systematic computational study of the distribution of the Fourier coefficients of cuspidal Hecke eigenforms of level $\Gamma_0(4)$ and half-integral weights. Based on substantial calculations, the question is raised whether the distribution of normalised Fourier coefficients with bounded indices can be approximated by a generalised Gaussian distribution. Moreover, it is argued that the apparent symmetry around zero of the data lends strong evidence to the Bruinier–Kohnen conjecture on the equidistribution of signs and even suggests the strengthening that signs and absolute values are distributed independently.

Key words: Modular forms of half-integer weight, Fourier coefficients of automorphic forms, Ramanujan–Petersson conjecture, Sato–Tate conjecture, distribution of coefficients, sign changes

1. Introduction

This article represents a systematic computational study of the Fourier coefficients of half-integral weight cuspidal Hecke eigenforms with the aim of experimentally shedding new light on their distribution, particularly focusing on signs.

Size and normalisation of coefficients and the Ramanujan–Petersson conjecture. Let $f = \sum_{n=1}^{\infty} a(n)q^n$ be a cuspidal Hecke eigenform of weight k. The Ramanujan–Petersson conjecture (see e.g., [30]) claims

$$a(n) = O(n^{(k-1)/2+\varepsilon})$$

for any $\varepsilon > 0$. By Deligne's famous proof of the Weil conjectures [16], the Ramanujan–Petersson conjecture is true with $\varepsilon = 0$ in the *integer* weight case. Motivated by the Ramanujan–Petersson conjecture we define the normalised coefficients to be

$$b(n) := \frac{a(n)}{n^{(k-1)/2}}.$$

It seems that the Ramanujan–Petersson conjecture has not been proved for a single cuspform of nonintegral weight. However, it is known by work of Gun and Kohnen in [18] that the Ramanujan–Petersson conjecture would fail for $\varepsilon = 0$ in half-integral weight. Their argument uses a sequence of nonsquarefree indices coming from the Shimura lift to construct a counter example. In recent work of Gun, Kohnen and Soundararajan [19],

*Correspondence: ilker.inam@bilecik.edu.tr; ilker.inam@gmail.com
2010 *AMS Mathematics Subject Classification:* 11F30 (primary); 11F37; 11F25

the authors suggest that in half-integral weight 'perhaps' the bound

$$|b(|n|)| \leq \exp(C\sqrt{\log|n| \log\log|n|}),$$

derived from conjectures in [17] and stronger than the stated form of the Ramanujan–Petersson conjecture might hold.

Known results and conjectures on the distribution in half-integral weight. In half-integral weight $k = \ell + \frac{1}{2}$, there is the crucial relation, due to Waldspurger (Theorem 1 on p. 378 of [41]) and Kohnen–Zagier (Theorem 1 of [31], p. 177), between the squares of the Fourier coefficients and central values of L-functions. More precisely, the Shimura lift (see [38] and [40]) relates those Fourier coefficients of f that are indexed by tn^2 with $t \in \mathbb{N}$ squarefree and $n \in \mathbb{N}$ to the n-th Fourier coefficient of a modular form g in integral weight 2ℓ. Then $b(|n|)^2$ is proportional to $L(g, \chi_n, \ell)$ for fundamental discriminants n such that $|n| = (-1)^\ell n$, where $L(g, \chi_n, s)$ is the Hecke L-function of g twisted by the primitive quadratic character χ_n corresponding to n.

This relation is at the basis of most of the results on the absolute value of $b(|n|)$ and has led to a conjectural description of the distribution of the $b(|n|)^2$ for fundamental discriminants n. In that context, we recall that the famous Sato–Tate conjecture describing the distribution of the normalised Fourier coefficients in the integral weight case has been proved by Barnet–Lamb, Geraghty, Harris and Taylor [11]. In [13], Conrey, Keating, Rubinstein and Snaith propose a conjecture on the distribution of coefficients of modular forms of weight $3/2$ attached to elliptic curves. Their Conjecture 4.2 states that for a modular form of weight $3/2$ which is attached to an elliptic curve E, the natural density of fundamental discriminants n such that

$$\alpha \leq (\kappa^{\pm}\sqrt{\log(|n|)}(b(|n|))^2)^{\frac{1}{\sqrt{\log\log|n|}}} \leq \beta$$

equals

$$\frac{1}{\sqrt{2\pi}} \int_\alpha^\beta \frac{1}{t} \exp(-\frac{1}{2}(\log t)^2)dt,$$

where $\kappa^{\pm}$ is a positive constant and $0 \leq \alpha \leq \beta$. K. Soundararajan kindly informed us that similar conjectures are made for higher weights as well. Note also that Conjecture 4.2 of [13] implies that the normalised coefficients $b(|n|)$ tend to zero almost surely, in the sense that for all $\varepsilon > 0$, the set of $d \in S^{\pm}$ such that $|b(|d|)| < \varepsilon$ has natural density equal to 1. This prediction is confirmed by a theorem of Radziwiłł and Soundararajan [39], as cited in [19] in level $\Gamma_0(4)$:

> *For every $\varepsilon > 0$, there is a constant $C = C(\varepsilon, f)$ such that for all but $o(x)$ fundamental discriminants n with $x \leq (-1)^\ell n \leq 2x$, one has*
>
> $$|b(|n|)| \leq C \cdot \log(|n|)^{-\frac{1}{4}+\varepsilon}. \tag{1.1}$$

This theorem hence implies that the normalised coefficients $b(n)$ tend to 0 with probability 1 and hence follow a Dirac distribution at 0. In the other direction, in recent work of Gun, Kohnen and Soundararajan [19], the existence of large values for normalised Fourier is proved (for level $\Gamma_0(4)$):

For any $\varepsilon > 0$ *and* x *large, there are at least* $x^{1-\varepsilon}$ *fundamental discriminants* n *with* $x < (-1)^{\ell} n < 2x$ *such that*

$$|b(|n|)| \geq \exp\left(\frac{1}{82}\frac{\sqrt{\log|n|}}{\sqrt{\log\log|n|}}\right). \tag{1.2}$$

Note that the relation with central values of L-functions only gives information about the squares of the coefficients and hence no information about their signs. This is where the conjecture of Bruinier and Kohnen ([10], [28]) enters, claiming that exactly half of the nonzero coefficients are positive, the other half negative.

At the heart of the signs problem on Fourier coefficients of modular forms of (half)-integer weights, there lie nonvanishing results such as [1], [2], [3], [4] and [5]. We note that there are also some interesting results on the (small) gaps between nonzero Fourier coefficients, for instance [14], [15], [32] and [33]. The sign change problem receives much attention and for example results [12] and [27] are in this direction. There are also more general results as in [34], [35] and one fundamental paper in another direction is [36]. Finally, there has been important recent progress on the distribution of the signs. In [37], the authors show for a Hecke eigenform in the Kohnen-plus space that $a(n)$ is negative for a positive proportion of fundamental discriminants n under the assumption of the Generalised Riemann Hypothesis, as well as a similar result for positive $a(n)$. In a continuation work, in [25] the authors generalize Theorem 1 of [19] and they extend the results of [37] to noneigenforms.

Contributions of this work. Here are the main points that we want to make with this article.

(1) Even though it is known by (1.1) that the absolute values of the normalised coefficients $b(|n|)$ tend to zero with probability 1, we do observe a very neat nontrivial distribution of the coefficients up to (computationally reachable) bounds. The distribution seems to follow a generalised Gaussian distribution.

(2) The histograms of the distribution of the normalised Fourier coefficients up to varying bounds and for varying Hecke eigenforms of half-integral weights all seem to present a similar 'global shape' in the sense that they can be well approximated by a single type of density function, and that only the parameters depend on the modular form and on the bound.

(3) The symmetry around 0 of the observed distributions of the coefficients up to bounds can be interpreted as very strong evidence towards the Bruinier–Kohnen conjecture. In fact, it suggests a strengthening of the conjecture to the point that the absolute value and the signs are independently distributed (see Conjecture 6.1). To the best of our knowledge, the calculations in this article can be seen as the most systematic and largest computational support for the Bruinier–Kohnen conjecture to date. Furthermore, if Question 5.1 has a positive answer then the Bruinier–Kohnen conjecture is true and this links the two topics in the title.

Short overview over the article. In §2, we report on the examples of half-integral weight modular cuspforms used for our experimental study and how they were computed. The main point is that we chose to stay in the lowest possible level $\Gamma_0(4)$ and considered weights up to $61/2$. In view of studying the distribution of the normalised Fourier coefficients of the examples, we created histograms and report on them in §3. We take into account the specific nature of half-integral weight forms that distinguishes them significantly from the well understood integral weight ones: we disregard all coefficients that via the Shimura lift come from the integral case and, consequently, study only squarefree indexed coefficients. The similar shape that the histograms exhibit suggests that they can be described by distribution functions. We consider four types of such functions in §4,

namely, the Laplace and the Cauchy distribution as well as two generalisations of the Gaussian distribution. We also report on data obtained when fitting the aforementioned distribution functions with the histograms. It turns out that one of the generalised Gaussian distributions is clearly the best one. In view of the fact that the normalised coefficients tend to zero almost surely, in §5 we explicitly seek for dependencies of the best fit parameters with data such as the number of coefficients used. We also formulate the explicit question if the normalised Fourier coefficients up to any bound indeed follow such a generalised Gaussian distribution, see Question 5.1. Finally, in §6, we recall the Bruinier–Kohnen conjecture and some previous results on it. We make the point that the observed symmetry of the histograms and of the studied distribution functions around zero is strong computational evidence in favour of the conjecture and even suggests a strengthening of it.

2. Examples of Hecke eigenforms in half-integral weights for $\Gamma_0(4)$

For studying their distribution computationally, we need as many Fourier coefficients of modular forms as possible. Since we are interested in higher weights, we choose to work in the smallest possible level $\Gamma_0(4)$. As described in the article [24] by two of the authors, the Kohnen-plus space in half-integral weight admits bases that can be computed relatively quickly up to some high precision. For this article, we worked with the Rankin–Cohen basis as described in loc. cit. We performed exact computations over the rationals in order not to lose any precision and only converted the normalised coefficients to real numbers in the end. A disadvantage of this choice is a huge consumption of memory, when the q-expansions are computed up to a high power of q.

To give some more details, we use Pari/GP* to express Hecke eigenforms with respect to the Rankin–Cohen basis. Here the *mf package* of Pari/GP [8] provides us with the necessary tools. Then, we export the basis coefficients to Magma [9], where we construct the Hecke eigenform as a power series (in general, over a number field). This is done in Magma because it provides very fast algorithms for the multiplication of power series. In a final step, we compute the normalised coefficients over the reals. Since all previous computations are exact computations, 10 digits of real precision are enough.

We only recorded coefficients at squarefree indices which are not known to be zero by the fact that we look only in the Kohnen-plus space (e.g., when $k-1/2$ is even, $a(n)$ is zero when n is 2 or 3 modulo 4). We also normalised all modular forms in such a way that the first recorded normalised coefficient equals 1. This is the natural way of normalisation if we consider the definition of the Kohnen-plus space, but it is in no way canonical.

We compute all Hecke eigenforms of weights $13/2, 17/2, 19/2, \ldots, 61/2$ (level $\Gamma_0(4)$) with 10^7 Fourier coefficients. By this, we mean all normalised coefficients $b(n)$ with squarefree index $n < 10^7$. We reached 10^8 Fourier coefficients for some examples and for the weight $13/2$, we could go up to $2 \cdot 10^8$. Text files containing the normalised coefficients can be downloaded†. The total amount of data used for the study exceeds 4 GB. In all tables below, a label such as $25/2(2)$ stands for the second cuspidal Hecke eigenform (with respect to an internal ordering) in weight $25/2$ and level $\Gamma_0(4)$. The reader is referred to [24] for some more details on the computations.

Note that, under the Shimura lift, any half-integral weight Hecke eigenform (in weight k) corresponds to an integral weight Hecke eigenform in level 1 and weight $2k-1 \in 2\mathbb{Z}$. By [29, p. 241], the Shimura lift is a Hecke equivariant isomorphism between the Kohnen plus space and the corresponding space in integral

*The PARI Group Univ. Bordeaux (2019). PARI/GP version2, 11.2 [online]. Website http://pari.math.u-bordeaux.fr/ [accessed 13.05.2021]

†http://math.uni.lu/wiese/FourierData.html

weight. This means that the eigenforms in half-integral weight are in bijection with those in integral weight. By Maeda's conjecture (see [21]), in weight $2k-1$ there is only a single Hecke orbit of eigenforms. Assuming Maeda's conjecture (which is known up to high weight by [20], far exceeding our examples), it follows that the number of half-integral weight Hecke eigenforms in the Kohnen-plus space equals the degree of the number field generated by the coefficients of the integral weight form.

3. Histograms for the distribution of normalised coefficients

The principal aim of this article is to understand the distribution of normalised coefficients of half-integral weight Hecke eigenforms. More precisely, the point we want to make is the following. Even though the normalised coefficients $b(n)$ tend to zero almost surely by the cited result of Radziwiłł and Soundararajan, the coefficients up to bounds that we can computationally reach do follow a very interesting non trivial distribution, which can be well approximated by density functions. They turn out to be symmetric around zero.

In order to study the distribution, we created histograms for the distribution of the normalised coefficients for all the modular forms mentioned in the previous section. We restricted our attention to coefficients with squarefree indices that are not known to be zero by the fact that the modular form lies in the Kohnen plus-space. The reason for only considering squarefree indices is the following: coefficients at indices of the form tn^2 with t squarefree and $n \in \mathbb{Z}_{\geq 2}$ are governed by the n-th coefficient of the Shimura lift, which is an integral weight eigenform and thus behaves with respect to the proved Sato-Tate law (if it is not CM). So, if we did not restrict to squarefree indices, we would 'mix' two distributions, making the pictures harder to analyse.

We created histograms for the distribution of the normalised coefficients using gnuplot [‡]. One choice that one has to make is that of the box size for the histograms. In order to understand dependencies, we created the histograms with different box sizes. Some box sizes are more pleasing to the eye than others (sometimes depending on the modular form). The graphs in Figure 1 are the histograms of the normalised Fourier coefficients $b(n)$ for the Hecke eigenform of weight $13/2$ with box sizes 0.001, 0.0001 and 0.00001, respectively, with 10^8 Fourier coefficients.

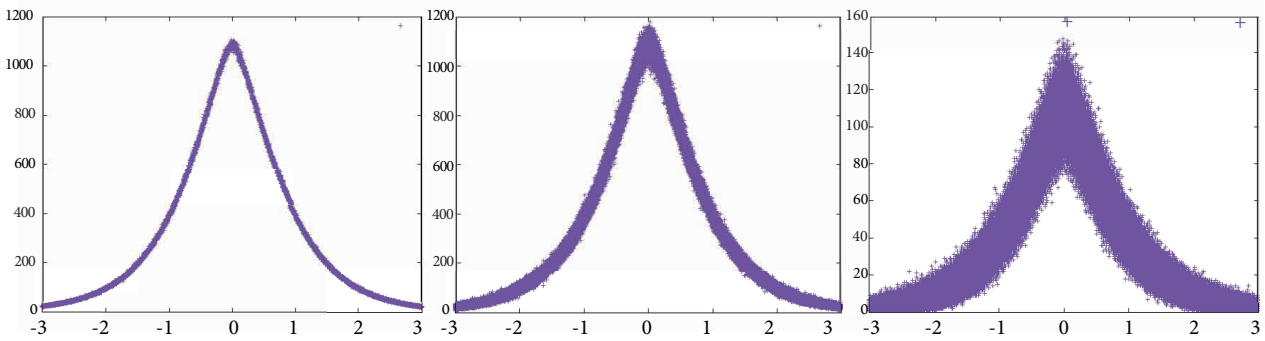

Figure 1. Histogram of 10^8 normalised Fourier coefficients of the Hecke eigenform of weight $13/2$ with box sizes 0.001, 0.0001 and 0.00001, respectively.

We observed that the choice of box size does not influence the parameters for best fits in any significant way. To confirm this, we give Table 1 for the parameter a for the GG-distribution for five different forms

[‡]Williams T, Kelley C (2017). Gnuplot 5.2: an interactive plotting program [online]. Website http://gnuplot.sourceforge.net/ [accessed 13.05.2021]

(indicated by their weights) and three different box widths. We hence disregard box sizes in our discussions and, throughout the paper, we use graphs with box size 0.001 since in this case, the graphs seem the most pleasing to the eyes.

Table 1. Best fit parameters with different box widths for the parameter a in the GG-distribution.

	0.001	0.0001	0.00001
13/2	0.634	0.634	0.633
17/2	0.553	0.553	0.553
21/2	0.558	0.558	0.557
25/2(1)	0.504	0.504	0.504
29/2(1)	0.506	0.506	0.506

4. Candidate distribution functions and fits

The point that we want to make in this section is the following: The 'global shape' of the histograms is independent of the modular form and of the bound for the coefficients. More precisely, our computations suggest that the histograms for the normalised Fourier coefficients of any half-integral weight Hecke eigenforms up to a given bound can be described by a single type of density function, and that only the parameters depend on the modular form as well as on the bound.

Looking at the histograms, one immediately notices that the histograms look symmetric around 0. Even though they present some kind of bell shape, one also sees very quickly that they do not follow a standard Gaussian. Instead, we tried the following two generalisations of the standard Gaussian and also the Laplace and the Cauchy distributions:

$$\mathsf{GGG}(x) := b \cdot \exp\left(-\frac{(d+x^2)^a}{c}\right) \tag{4.1}$$

$$\mathsf{GG}(x) := b \cdot \exp\left(-\frac{(x^2)^a}{c}\right) \tag{4.2}$$

$$\mathsf{Laplace}(x) := b \cdot \exp(-|x|/c) \tag{4.3}$$

$$\mathsf{Cauchy}(x) := \frac{a}{b+(cx)^2}. \tag{4.4}$$

Of course, GG is a special case of GGG (with $d = 0$) and $\mathsf{Laplace}$ is a special case of GG (with $a = 0.5$). Since the a-parameter in GG is quite close to 0.5 (the data is given in Appendix 6) and because the Laplace distribution is much simpler than the generalised Gaussian, we took it up into our considerations. Since we did not normalise our histograms so that the area under it is 1, we also did not normalise the above distribution functions to be probability distributions (even though we think of them this way).

Graphically, all four distribution functions describe the histograms pretty well, the GGG-distribution being clearly the best. The Cauchy distribution seems to be systematically too high in the tails, whence we consider it the worst of the four. The reader is referred to Appendix 6 for the graphs with inscribed best fit distribution functions. Sample graphs of some fits are given in Figures 2-4.

Since our histograms are not uniformly normalised (recall that we normalised the coefficients of the half-integral weight form in such a way that the first nonzero coefficient is 1) in the sense that generally they present the same shape, but some are wider, some are steeper, etc., it is very hard to compare the quality of the fits

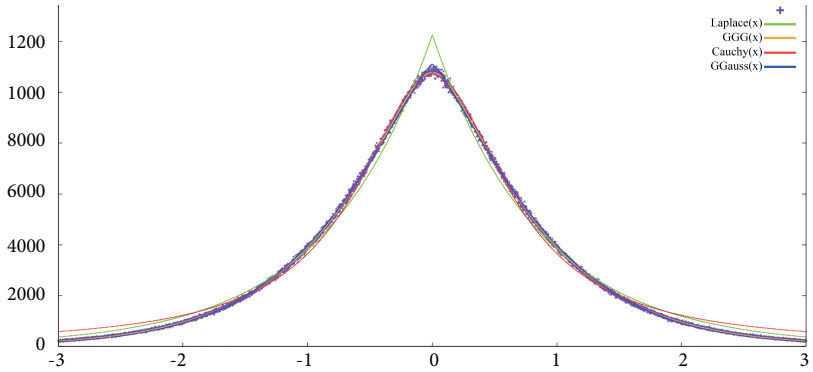

Figure 2. Histogram and distributions of Hecke eigenform of weight $13/2$ with 10^8 coefficients.

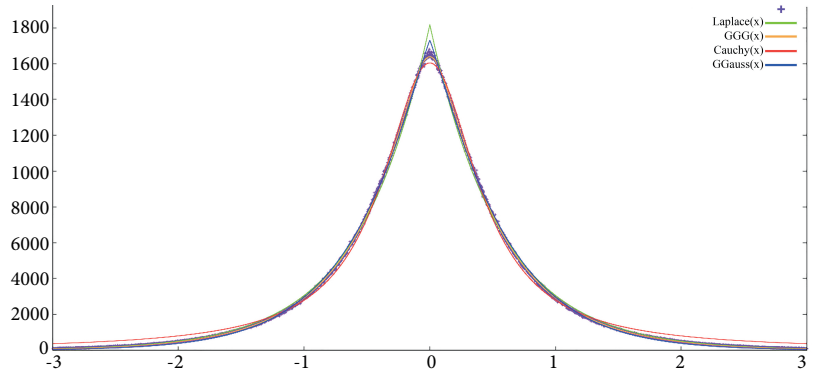

Figure 3. Histogram and distributions of Hecke eigenform of weight $25/2$ with 10^8 coefficients.

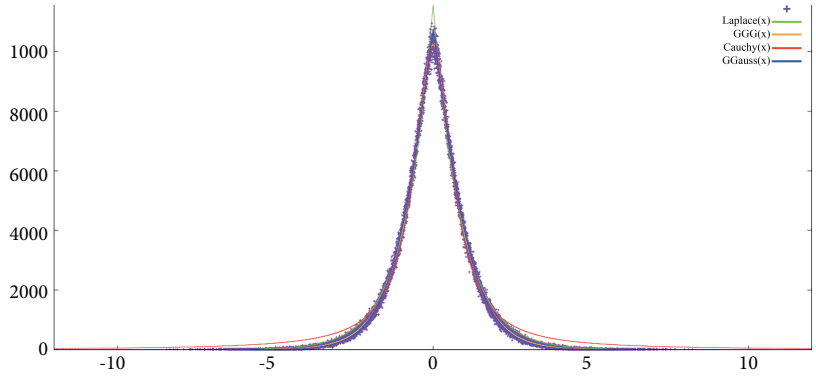

Figure 4. Histogram and distributions of the second Hecke eigenform of weight $43/2$ with 10^7 coefficients.

between different histograms. We will measure the quality of the fits by the root mean square (RMS) value as output by gnuplot. Of course, the GGG-fit will always be better than the GG-fit and that one will always be better than the Laplace-fit as they are special cases of each other.

We illustrate the results of the fits performed using gnuplot by giving in Table 2 all best fit values for all examples for which we reached 10^8 Fourier coefficients. The results for computations up to 10^7 Fourier coefficients are included in Appendix 6.

5. Dependence or independence of parameters

Even though the distribution for normalised coefficients up to the bounds we reached computationally can be pretty well described by the GGG function, as seen in the previous section, the result of Radziwiłł and Soundararajan shows that, for a fixed Hecke eigenform, the parameters must depend on the bound. We investigate this dependence in this section. More precisely, we look at how the parameters behave with respect to x, when we compute with all coefficients up to x.

In order to study this, we consider the case where we have the biggest number of normalised Fourier coefficients, namely $2\cdot 10^8$, in weight $13/2$. We broke the list of coefficients into 20 subsequent lists of equal size and did the fitting for each of these sublists separately, leading to the results in Table 3. One clearly observes some dependence. For instance, for the Laplace distribution (4.3), the b value seems to be slowly, but strictly increasing, whereas the c-value slowly, but strictly decreases (with one exception). The values for the Cauchy distribution (4.4) and the GG-distribution (4.2) also suggest a dependence. For the GGG-distribution (4.1), there is a clear dependence of the values for the first couple of sets. However, all four values seem to stabilise for the last sets. The range of data we investigated hence does not allow us to illustrate that the limit distribution is known to be a Dirac delta function.

Recall that we restricted our efforts to squarefree indices n such that the coefficient is not automatically known to be zero. We investigated further if the distribution seems to change significantly when considering prime indexed coefficients only. In the integral weight case, there are huge differences and the semicircular distribution of Sato–Tate for non-CM eigenforms is only valid for prime indices. Moreover, the coefficients of integral weight Hecke eigenforms are multiplicative functions, hence the distribution of the coefficients at prime indices determines the rest. We do not know of any reason to believe that similar things happen in the half-integral weight case. Indeed, the shapes of the distribution graphs do not change significantly if we restrict to prime indices (see Figure 5 for an example). Of course, some of the best fit parameters move, as we can see in Table 4: The b values differ just because there are far more squarefree numbers than prime numbers. For the same reason also the RMS values are different. However, the most important parameters, i.e. the a-parameters in GGG and GG are very similar. It is not clear if the slight change of parameters can be explained by the fact that the set of primes among squarefree numbers is biassed towards small values, or if the change is not significant. This gives us confidence in our belief that prime indexed normalised coefficients are not distributed differently from those with squarefree indices, when considering coefficients with indices up to the bounds we could reach.

The observed very good approximations by the GGG-distribution of the normalised Fourier coefficients up to the bounds we could computationally reach lead us to ask the question whether this holds for all bounds.

Question 5.1 *Let* f *be a half-integral weight cuspidal Hecke eigenform in the Kohnen plus-space in half-integral weight* $\mathsf{k}=\ell+\frac{1}{2}$ *and let* $\mathsf{b}(\mathsf{n})$ *be its normalised coefficients. Let* $\mathsf{x}\in\mathbb{R}_{>0}$.

Can the distribution of the $\mathsf{b}(\mathsf{n})$ *for* $\mathsf{n}\le\mathsf{x}$ *squarefree and* $\mathsf{n}\equiv(-1)^{\ell} \mod 4$ *be approximated by the* GGG*-distribution with parameters depending on* f *and* x*?*

More precisely, are there constants $\mathsf{a},\mathsf{c},\mathsf{d}$, *depending on* f *and* x, *such that for all intervals* $\mathsf{I}=[\alpha,\beta]\subseteq\mathbb{R}$ *the quotient*

$$\frac{\#\{\mathsf{n}\in\mathbb{R}\text{ squarefree}\mid \mathsf{n}\le\mathsf{x},\mathsf{n}\equiv(-1)^{\ell} \mod 4,\mathsf{b}(\mathsf{n})\in\mathsf{I}\}}{\#\{\mathsf{n}\in\mathbb{N}\text{ squarefree}\mid \mathsf{n}\le\mathsf{x},\mathsf{n}\equiv(-1)^{\ell} \mod 4\}}$$

is 'close to'

$$\frac{1}{b}\int_{\alpha}^{\beta} \exp(-\frac{(d+t^2)^a}{c})dt,$$

where $b = \int_{-\infty}^{\infty} \exp(-\frac{(d+t^2)^a}{c})dt$ *?*

Table 2.

Best fit parameters (rounded) for the GGG-distribution:

	a	b	c	d
13/2	0.581	12538	0.872	0.030
17/2	0.453	20421	0.550	0.030
19/2	0.385	44105	0.317	0.012
21/2	0.460	23411	0.485	0.022
23/2	0.494	14866	0.725	0.034
25/2(1)	0.391	19462	0.577	0.035
25/2(2)	0.237	88927	0.284	0.033
27/2	0.513	22681	0.471	0.014
29/2(1)	0.364	11886	0.812	0.092
29/2(2)	0.423	30278	0.402	0.016

Best fit parameters (rounded) for the GG-distribution:

	a	b	c
13/2	0.634	11105	0.969
17/2	0.553	14999	0.663
19/2	0.515	26822	0.363
21/2	0.558	17300	0.566
23/2	0.573	11997	0.857
25/2(1)	0.504	13107	0.752
25/2(2)	0.453	20676	0.485
27/2	0.584	18721	0.514
29/2(1)	0.506	7555	1.256
29/2(2)	0.532	20884	0.466

Best fit parameters (rounded) for the Laplace distribution:

	b	c
13/2	12264	0.860
17/2	15711	0.650
19/2	27201	0.367
21/2	18184	0.560
23/2	12746	0.805
25/2(1)	13161	0.750
25/2(2)	19699	0.484
27/2	20071	0.514
29/2(1)	7597	1.244
29/2(2)	21515	0.470

Best fit parameters (rounded) for the Cauchy distribution:

	a	b	c
13/2	183	0.017	0.181
17/2	194	0.014	0.222
19/2	2455	0.010	0.340
21/2	194	0.012	0.240
23/2	208	0.019	0.204
25/2(1)	194	0.017	0.212
25/2(2)	1376	0.080	0.725
27/2	233	0.013	0.272
29/2(1)	813	0.122	0.340
29/2(2)	342	0.018	-0.350

RMS values:

	GG	GGG	Laplace	Cauchy
13/2	76	59	286	252
17/2	126	64	187	219
19/2	208	75	215	295
21/2	133	66	209	265
23/2	97	60	190	189

	GG	GGG	Laplace	Cauchy
25/2(1)	134	62	135	178
25/2(2)	283	79	320	238
27/2	111	63	266	347
29/2(1)	95	56	95	157
29/2(2)	161	65	191	273

Table 3.

	GGG				GG			Laplace		Cauchy		
	a	b	c	d	a	b	c	b	c	a	b	c
1	0.622	1177	0.967	0.045	0.677	1038	1.08	1172	0.908	142.8	0.140	0.488
2	0.601	1206	0.917	0.031	0.650	1082	1.009	1205	0.876	142.0	0.135	0.498
3	0.591	1221	0.896	0.027	0.638	1101	0.981	1219	0.864	143.4	0.135	0.506
4	0.587	1230	0.886	0.025	0.633	1110	0.969	1226	0.858	144.1	0.135	0.510
5	0.569	1299	0.846	0.037	0.631	1117	0.960	1232	0.852	144.3	0.134	0.513
6	0.580	1252	0.867	0.025	0.627	1123	0.952	1236	0.848	144.8	0.134	0.515
7	0.561	1326	0.828	0.039	0.628	1126	0.948	1239	0.846	144.8	0.134	0.516
8	0.566	1292	0.841	0.030	0.622	1133	0.940	1243	0.843	145.6	0.134	0.520
9	0.572	1273	0.850	0.026	0.621	1136	0.936	1246	0.840	145.6	0.134	0.520
10	0.559	1317	0.825	0.032	0.619	1141	0.930	1249	0.837	146.0	0.134	0.522
11	0.567	1289	0.839	0.027	0.619	1141	0.930	1250	0.837	146.0	0.134	0.522
12	0.559	1317	0.824	0.031	0.618	1144	0.926	1252	0.835	146.2	0.133	0.523
13	0.557	1326	0.819	0.032	0.617	1146	0.924	1254	0.833	146.4	0.133	0.524
14	0.566	1275	0.840	0.020	0.610	1154	0.915	1257	0.830	147.3	0.134	0.524
15	0.551	1349	0.807	0.034	0.616	1150	0.919	1257	0.830	146.6	0.133	0.526
16	0.555	1332	0.814	0.031	0.616	1151	0.918	1258	0.828	146.5	0.133	0.526
17	0.555	1327	0.814	0.029	0.613	1156	0.913	1261	0.828	146.9	0.133	0.528
18	0.560	1309	0.822	0.025	0.612	1158	0.911	1262	0.826	147.0	0.133	0.529
19	0.553	1333	0.811	0.029	0.612	1157	0.911	1262	0.827	147.1	0.133	0.529
20	0.555	1323	0.814	0.026	0.610	1161	0.907	1264	0.825	147.3	0.133	0.530

Table of the corresponding RMS-values.

	GGG	GG	Laplace	Cauchy
1	18.4	18.9	39.0	33.6
2	18.1	18.6	35.4	31.6
3	18.7	19.2	34.1	31.2
4	18.2	18.8	33.3	30.7
5	18.0	18.8	33.2	30.0
6	18.5	19.0	32.7	30.4
7	18.4	19.3	33.0	29.9
8	18.2	19.0	31.9	29.7
9	18.3	18.8	31.7	29.9
10	18.3	19.1	31.6	29.5
11	18.4	19.0	31.6	29.8
12	18.3	19.2	31.5	29.5
13	18.3	19.2	31.5	29.5
14	18.2	18.7	30.1	29.4
15	17.7	18.7	31.0	28.9
16	18.3	19.2	31.3	29.4
17	18.0	18.8	30.6	29.1
18	18.3	19.0	30.7	29.4
19	18.4	19.2	30.8	29.2
20	18.4	19.2	30.5	29.2

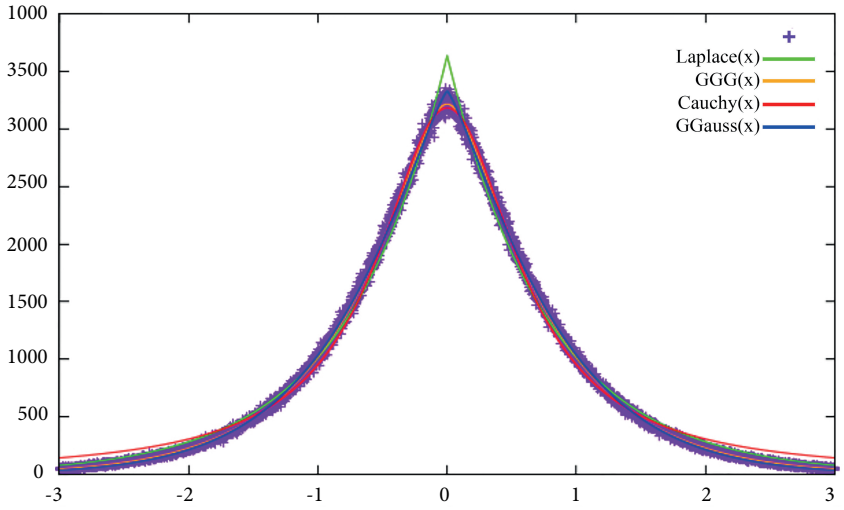

Figure 5. Histogram and distributions of Hecke eigenform of weight $13/2$ for prime indexed coefficients only.

Table 4.

	GGG				GG			Laplace		Cauchy		
	a	b	c	d	a	b	c	b	c	a	b	c
Sqfree	0.570	25666	0.850	0.030	0.623	22621	0.942	24837	0.843	140	0.006	0.113
Prime	0.550	3892	0.759	0.030	0.614	3329	0.856	3635	0.784	196	0.062	0.380

6. A strengthening of the Bruinier–Kohnen conjecture

Bruinier and Kohnen conjectured that the signs of coefficients of half-integral weight Hecke eigenforms are equidistributed. More precisely, let $f = \sum_{n=1}^{\infty} a(n)q^n \in S_k(N,\chi)$ be a cusp form of weight $k = \ell + 1/2$ with real Fourier coefficients and assume that f is orthogonal to the unary theta series when $\ell = 1$. Then the Bruinier–Kohnen conjecture ([10] and [28]) asserts that the sets $\{n \in \mathbb{N} : a(n) > 0\}$ and $\{n \in \mathbb{N} : a(n) < 0\}$ have the same natural density, equal to half of the natural density of $\{n \in \mathbb{N} : a(n) \neq 0\}$.

Combining the Shimura lift with the (proved) celebrated Sato–Tate conjecture for integral weight Hecke eigenforms, it is not very difficult to prove equidistribution of signs for the coefficients indexed by squares, see [6], [22], [23]. The sign equidistribution problem has still received much attention and is widely studied (for instance [7]), and the technique from [22] has been extended to more general automorphic forms like Hilbert modular forms in [26]. Note that this is only a partial result and the full proof of the conjecture is still an open problem and, for the moment, it is likely that there is no theoretical tool to attack this problem.

We see the calculations in this article as the most systematic and largest computational support for the Bruinier–Kohnen conjecture to date. In fact, if the distribution of coefficients up to any bound x follows any distribution function (depending on x) that is symmetric with respect to 0, e.g., any of the four types discussed above, then the Bruinier–Kohnen conjecture is true.

In fact, the symmetry around 0 suggests that the signs are uniformly distributed and that the distribution of the signs and the distribution of the absolute value of the normalised coefficients are independent. In order to make this precise, we recall that according to (1.2), there are infinitely many 'big' normalised coefficients

$|\mathsf{b}(\mathsf{n})|$. This suggests that any nonempty interval $\mathsf{I} \subseteq \mathbb{R}_{>0}$ will contain infinitely many normalised coefficients $|\mathsf{b}(\mathsf{n})|$ for squarefree n. We insist on squarefree because we do not want to deal with the contributions that are understood by the Shimura lift.

We feel that the symmetry around 0 of the distribution of the normalised coefficients up to the bounds that we computationally reached warrant the formulation of the following conjecture, strengthening the Bruinier–Kohnen conjecture.

Conjecture 6.1 (Independence of sign and absolute value) *Let* f *be as above. Let* $\mathsf{I} \subseteq \mathbb{R}_{>0}$ *be any interval. Then the following limit exists and we have*

$$\lim_{\mathsf{x}\to\infty} \frac{\#\{\mathsf{n} \leq \mathsf{x} \text{ squarefree } \mid |\mathsf{b}(\mathsf{n})| \in \mathsf{I}, \mathsf{b}(\mathsf{n}) > 0\}}{\#\{\mathsf{n} \leq \mathsf{x} \text{ squarefree } \mid |\mathsf{b}(\mathsf{n})| \in \mathsf{I}\}} = \frac{1}{2}.$$

Acknowledgment

This work is supported by the Scientific and Technological Research Council of Turkey (TÜBİTAK) with the project number 118F148. İ.İ. acknowledges partial and complement support by Bilecik Şeyh Edebali University research project number 2018-01.BSEU.04-01 and would like to thank the University of Luxembourg for the great hospitality in several visits. The authors thank the İzmir Institute of Technology and especially Prof. Dr. Engin Büyükaşık, where a huge part of this research was carried out, for its great hospitality.

The authors are extremely grateful to Kannan Soundararajan for very useful feedback on a first version of this article, clarifying various points to them. They also thank Henri Cohen for providing them with the initial code for obtaining Hecke eigenforms via Rankin–Cohen brackets in Pari/GP and Winfried Kohnen for interesting discussions. They also thank Oktay Pashaev for some interesting suggestions. Thanks are also due to the anonymous referees for helpful suggestions concerning the presentation of the paper. İ.İ. wishes to thank his parents who welcomed him during his İzmir visit in summer 2019. G.W. thanks Giovanni Peccati for suggesting the generalised Gaussian distribution.

References

[1] Alkan E. Nonvanishing of Fourier coefficients of modular forms. Proceedings of the American Mathematical Society 2003; 131: 1673-1680.

[2] Alkan E. On the sizes of gaps in the Fourier expansion of modular forms. Canadian Journal of Mathematics 2005; 57: 449-470.

[3] Alkan E, Zaharescu A. Nonvanishing of Fourier coefficients of newforms in progressions, Acta Arithmetica 2005; 116: 81-98.

[4] Alkan E, Zaharescu A. Nonvanishing of the Ramanujan tau function in short intervals, International Journal of Number Theory 2005; 1: 45-51.

[5] Alkan E, Ford K, Zaharescu A. Diophantine approximation with arithmetic functions. II., Bulletin of the London Mathematical Society 2009; 41: 676-682.

[6] Arias-de-Reyna S, Inam I, Wiese G. On conjectures of Sato-Tate and Bruinier-Kohnen. The Ramanujan Journal 2015; 36 (3): 455-481.

[7] Amri MA. Oscillatory behavior and equidistribution of signs of Fourier coefficients of cusp forms. The Ramanujan Journal 2019; 50 (3): 505-526.

[8] Belabas K, Cohen H. Modular forms in Pari/GP. Research in the Mathematical Sciences 2018; 5 (3): Paper No. 37, 19.

[9] Bosma W, Cannon J, Playoust C. The Magma algebra system. I. The user language. Journal of Symbolic Computation 1993; volume 24, pages 235-265. 1997. Computational algebra and number theory.

[10] Bruinier JH, Kohnen W. Sign changes of coefficients of half integral weight modular forms. In: Edixhoven B (editor). Modular forms on Schiermonnikoog, Cambridge: Cambridge Univ. Press 2008, pages 57-65.

[11] Barnet-Lamb T, Geraghty D, Harris M, Taylor R. A family of Calabi-Yau varieties and potential automorphy II. Publications of the Research Institute for Mathematical Sciences 2011; 47 (1): 29-98.

[12] Choie YJ, Kohnen W. The first sign change of Fourier coefficients of cusp forms, American Journal of Mathematics 2009; 131: 517-543.

[13] Conrey JB, Keating JP, Rubinstein MO, Snaith NC. Random matrix theory and the Fourier coefficients of half-integral weight forms. Experimental Mathematics 2006; 15 (1): 6-–82.

[14] Das S, Ganguly S. Gaps between nonzero Fourier coefficients of cusp forms, Proceedings of the American Mathematical Society 2014; 142: 3747-3755.

[15] Das S, Ganguly S. A note on small gaps between nonzero Fourier coefficients of cusp forms, Proceedings of the American Mathematical Society 2016; 144: 2301-2305.

[16] Deligne P. La conjecture de Weil. I. Publications mathématiques de l'Institut des Hautes Études Scientifiques 1974; (43): 273-307.

[17] Farmer DW, Gonek SM, Hughes CP. The maximum size of L-functions. Journal für die Reine Angewandte Mathematik 2007; 609: 215-236.

[18] Gun S, Kohnen W. On the Ramanujan-Petersson conjecture for modular forms of half-integral weight. Forum Mathematicum 2019; 31 (3): 703-711.

[19] Gun S, Kohnen W, Soundararajan K. Large Fourier coefficients of half-integer weight modular forms, ArXiv:2004.14450; 2020.

[20] Ghitza A, McAndrew A. Experimental evidence for Maeda's conjecture on modular forms. Tbilisi Mathematical Journal 2012; 5 (2): 55-69.

[21] Hida H, Maeda Y. Non-abelian base change for totally real fields. Pacific Journal of Mathematics 1997; Vol. 181, No. 3, pages 189-217.

[22] Inam I, Wiese G. Equidistribution of signs for modular eigenforms of half integral weight. Archiv der Mathematik (Basel) 2013; 101 (4): 331-339.

[23] Inam I, Wiese G. A short note on the Bruiner-Kohnen sign equidistribution conjecture and Halász' theorem. International Journal of Number Theory 2016; 12 (2): 357-360.

[24] Inam I, Wiese G. Fast computation of half-integral weight modular forms. preprint, 2020.

[25] Jääsaari J, Lester S, Saha A. On fundamental Fourier coefficients of Siegel cusp forms of degree 2, ArXiv:2012.09563, 2020.

[26] Kaushik S, Kumar N, Tanabe N. Equidistribution of signs for Hilbert modular forms of half-integral weight. Research in Number Theory 2018; 4 (2):Paper No. 13,10.

[27] Kohnen W, Lau YK, Shparlinski IE. On the number of sign changes of Hecke eigenvalues of newforms, Journal of the Australian Mathematical Society 2008; 85: 87-94.

[28] Kohnen W, Lau YK, Wu J. Fourier coefficients of cusp forms of half-integral weight. Mathematische Zeitschrift 2013; 273 (1-2): 29-41.

[29] Kohnen W. Fourier coefficients of modular forms of half-integral weight. Mathematische Annalen 1985; 271 (2): 237-268.

[30] Kohnen W. On the Ramanujan-Petersson conjecture for modular forms of half-integral weight. Proceedings of the Indian Academy of Sciences: Mathematical Sciences 1994; 104(2): 333–337.

[31] Kohnen W, Zagier D. Values of L-series of modular forms at the center of the critical strip. Inventiones Mathematicae 1981; 64 (2): 175–198.

[32] Kumar N. On the gaps between non-zero Fourier coefficients of cusp forms of higher weight, The Ramanujan Journal 2018; 45: 95-109.

[33] Kumar N. Kaushik S. On the gaps between non-zero Fourier coefficients of eigenforms with CM, International Journal Number Theory 2018; 14: 95-101.

[34] Kumar N. Kaushik S. Simultaneous behavior of the Fourier coefficients of two Hilbert modular cusp forms, Acta Arithmetica 2019; 112: 241-248.

[35] Kumar N. A variant of multiplicity one theorems for half integral weight modular forms, Acta Arithmetica 2019; 190: 75-85.

[36] Murty MR. Oscillations of Fourier coefficients of modular forms, Mathematische Annalen 1983; 262: 431-446.

[37] Lester S, Radziwiłł M. Signs of Fourier coefficients of half integral weight modular forms. Mathematische Annalen 2021; 379: 1553-1604.

[38] Niwa S. Modular forms of half integral weight and the integral of certain theta functions. Nagoya Mathematical Journal 1975; 56: 147-161.

[39] Radziwiłł M, Soundararajan K. Moments and distribution of central L-values of quadratic twists of elliptic curves. Inventiones Mathematicae 2015; 202 (3): 1029-1068.

[40] Shimura G. On modular forms of half integral weight. Annals of Mathematics 1973; (2): 97: 440–481.

[41] Waldspurger JL. Sur les coefficients de Fourier des formes modulaires de poids demi-entier. Journal de Mathématiques Pures et Appliquées 1981; (9): 60 (4): 375-484.

Appendix: Graphs of histograms of all computed examples

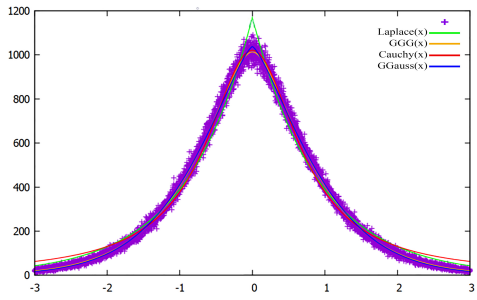

Figure A1. Histogram of 10^7 normalised Fourier coefficients of Hecke eigenform of weight 13/2 and distributions

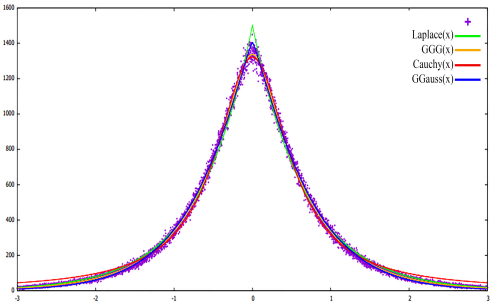

Figure A2. Histogram of 10^7 normalised Fourier coefficients of Hecke eigenform of weight 17/2 and distributions

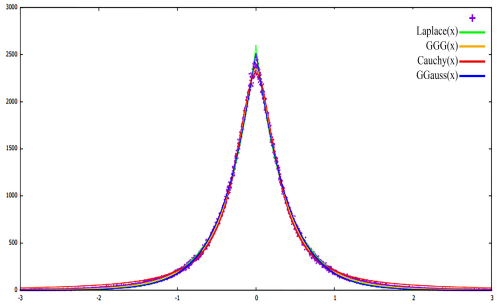

Figure A3. Histogram of 10^7 normalised Fourier coefficients of Hecke eigenform of weight 19/2 and distributions

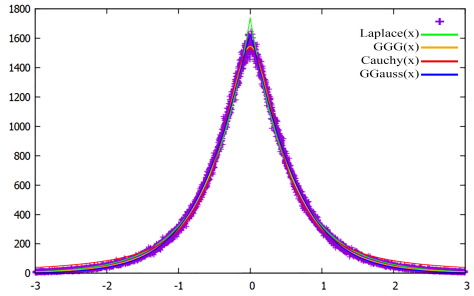

Figure A4. Histogram of 10^7 normalised Fourier coefficients of Hecke eigenform of weight 21/2 and distributions

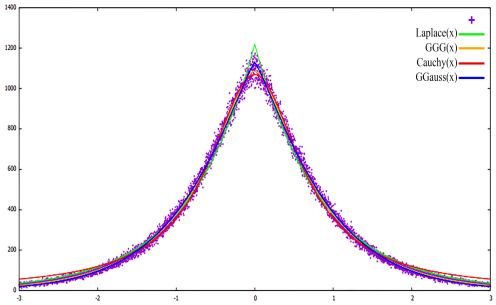

Figure A5. Histogram of 10^7 normalised Fourier coefficients of Hecke eigenform of weight 23/2 and distributions

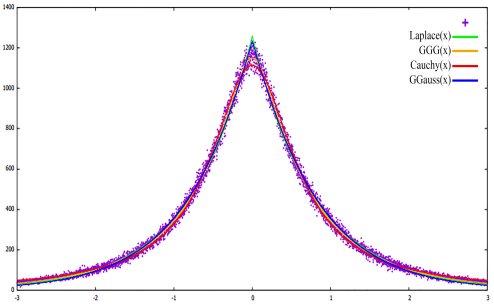

Figure A6. Histogram of 10^7 normalised Fourier coefficients of first Hecke eigenform of weight 25/2 and distributions

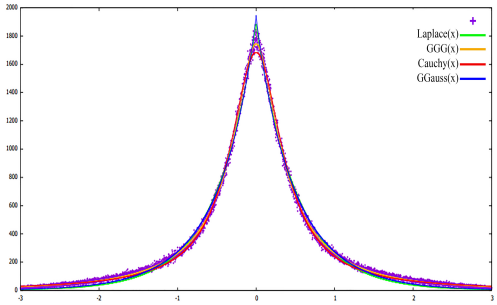

Figure A7. Histogram of 10^7 normalised Fourier coefficients of second Hecke eigenform of weight $25/2$ and distributions

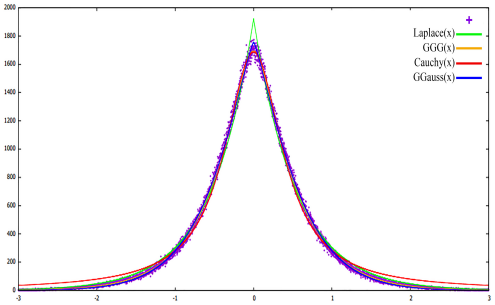

Figure A8. Histogram of 10^7 normalised Fourier coefficients of Hecke eigenform of weight $27/2$ and distributions

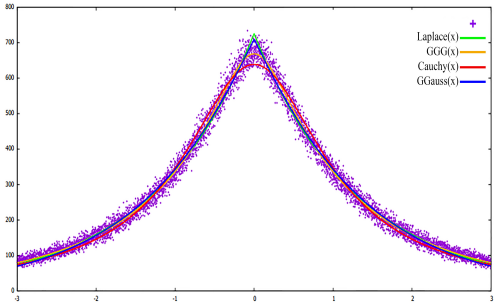

Figure A9. Histogram of 10^7 normalised Fourier coefficients of Hecke eigenform of weight $29/2$ and distributions

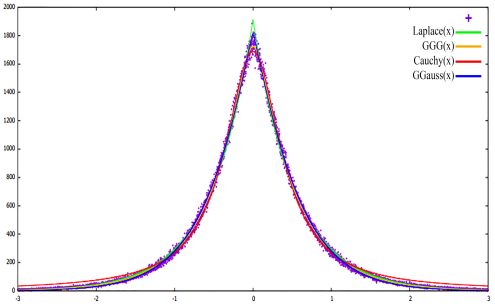

Figure A10. Histogram of 10^7 normalised Fourier coefficients of first Hecke eigenform of weight $31/2$ and distributions

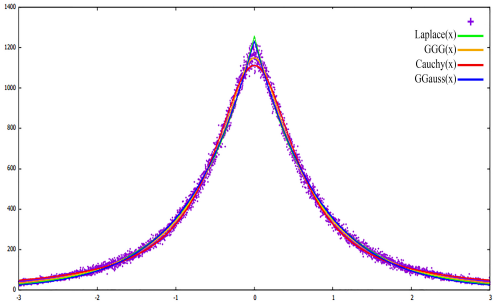

Figure A11. Histogram of 10^7 normalised Fourier coefficients of second Hecke eigenform of weight $31/2$ and distributions

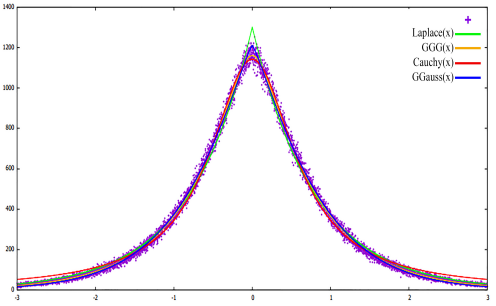

Figure A12. Histogram of 10^7 normalised Fourier coefficients of first Hecke eigenform of weight $33/2$ and distributions

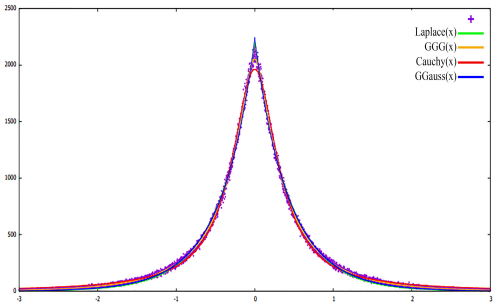

Figure A13. Histogram of 10^7 normalised Fourier coefficients of second Hecke eigenform of weight $33/2$ and distributions

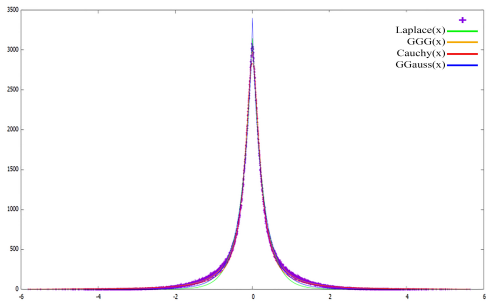

Figure A14. Histogram of 10^7 normalised Fourier coefficients of first Hecke eigenform of weight $35/2$ and distributions

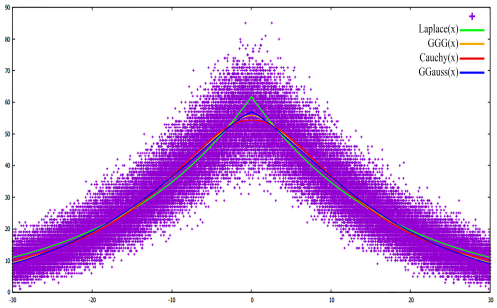

Figure A15. Histogram of 10^7 normalised Fourier coefficients of second Hecke eigenform of weight $35/2$ and distributions

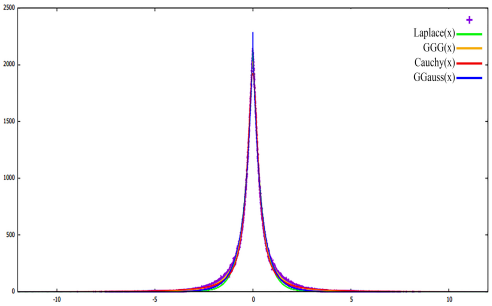

Figure A16. Histogram of 10^7 normalised Fourier coefficients of first Hecke eigenform of weight $37/2$ and distributions

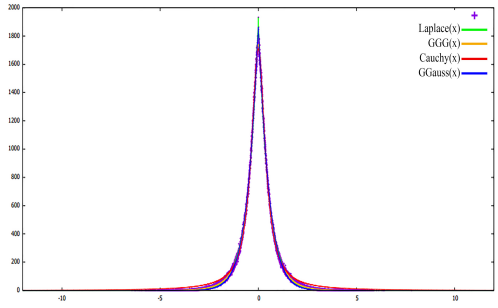

Figure A17. Histogram of 10^7 normalised Fourier coefficients of second Hecke eigenform of weight $37/2$ and distributions

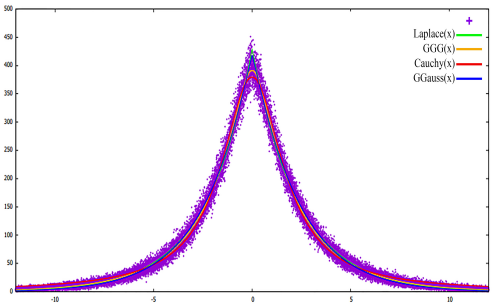

Figure A18. Histogram of 10^7 normalised Fourier coefficients of third Hecke eigenform of weight $37/2$ and distributions

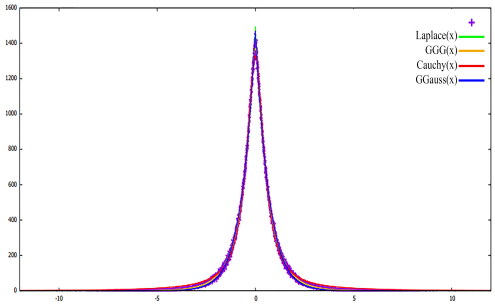

Figure A19. Histogram of 10^7 normalised Fourier coefficients of first Hecke eigenform of weight $39/2$ and distributions

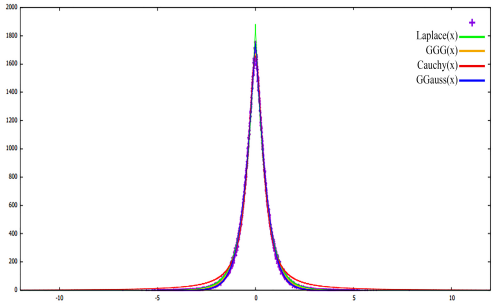

Figure A20. Histogram of 10^7 normalised Fourier coefficients of second Hecke eigenform of weight $39/2$ and distributions

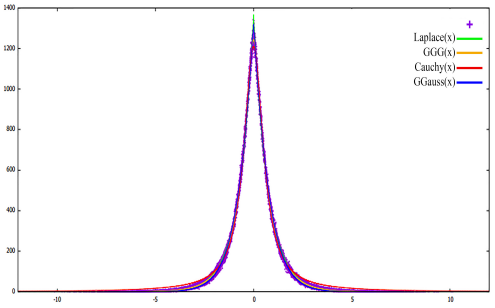

Figure A21. Histogram of 10^7 normalised Fourier coefficients of first Hecke eigenform of weight $41/2$ and distributions

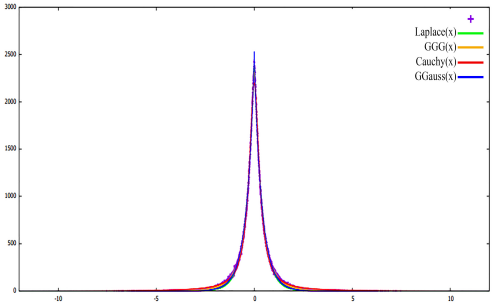

Figure A22. Histogram of 10^7 normalised Fourier coefficients of second Hecke eigenform of weight $41/2$ and distributions

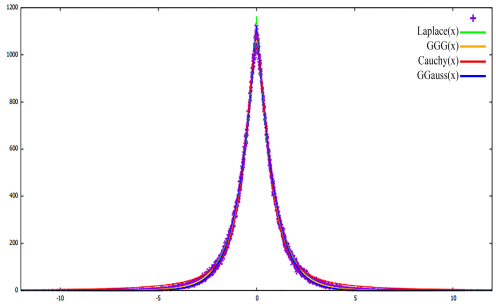

Figure A23. Histogram of 10^7 normalised Fourier coefficients of third Hecke eigenform of weight $41/2$ and distributions

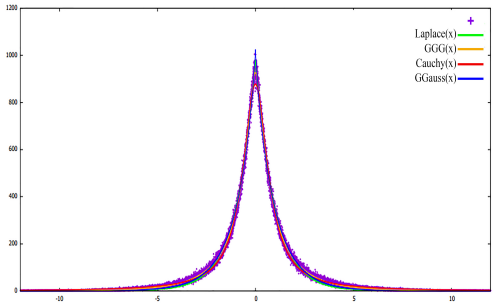

Figure A24. Histogram of 10^7 normalised Fourier coefficients of first Hecke eigenform of weight $43/2$ and distributions

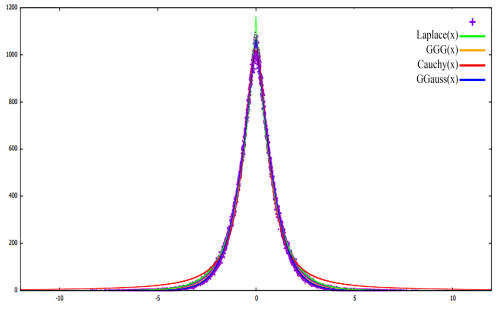

Figure A25. Histogram of 10^7 normalised Fourier coefficients of second Hecke eigenform of weight $43/2$ and distributions

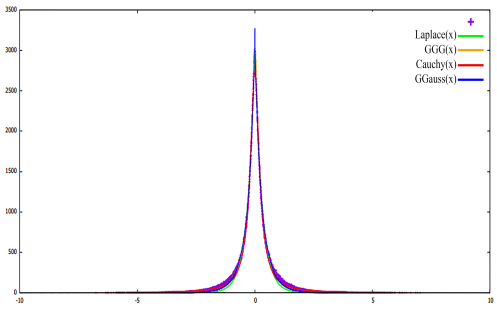

Figure A26. Histogram of 10^7 normalised Fourier coefficients of third Hecke eigenform of weight $43/2$ and distributions

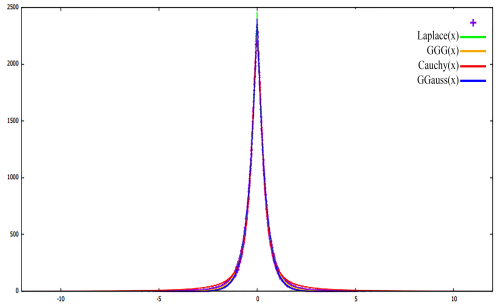

Figure A27. Histogram of 10^7 normalised Fourier coefficients of first Hecke eigenform of weight $45/2$ and distributions

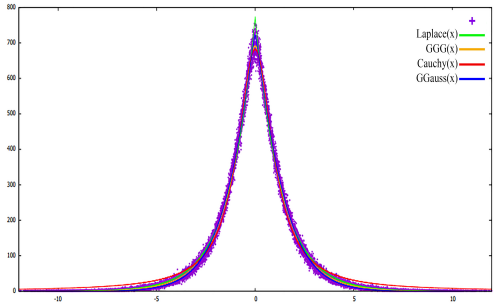

Figure A28. Histogram of 10^7 normalised Fourier coefficients of second Hecke eigenform of weight $45/2$ and distributions

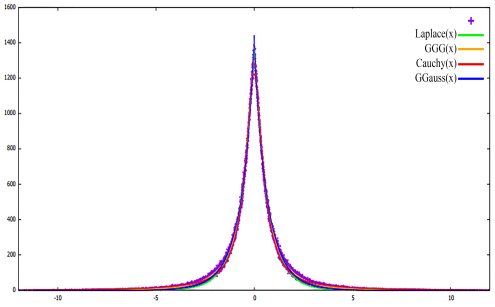

Figure A29. Histogram of 10^7 normalised Fourier coefficients of third Hecke eigenform of weight $45/2$ and distributions

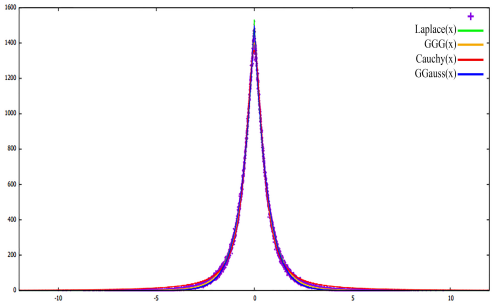

Figure A30. Histogram of 10^7 normalised Fourier coefficients of first Hecke eigenform of weight $47/2$ and distributions

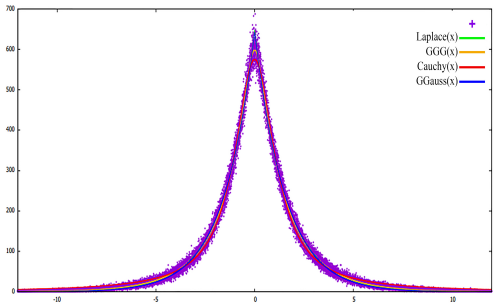

Figure A31. Histogram of 10^7 normalised Fourier coefficients of second Hecke eigenform of weight $47/2$ and distributions

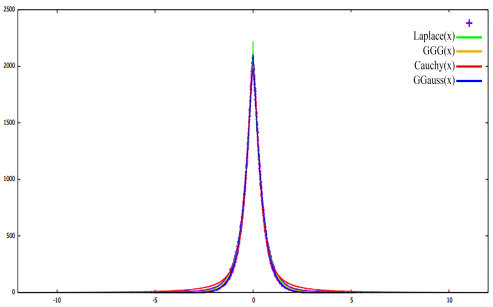

Figure A32. Histogram of 10^7 normalised Fourier coefficients of third Hecke eigenform of weight $47/2$ and distributions

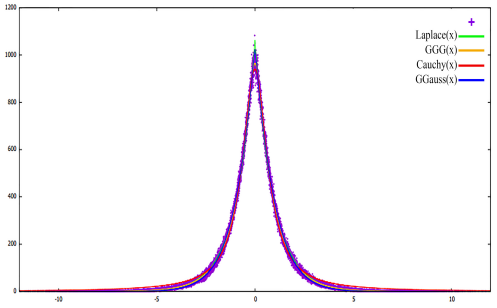

Figure A33. Histogram of 10^7 normalised Fourier coefficients of first Hecke eigenform of weight $49/2$ and distributions

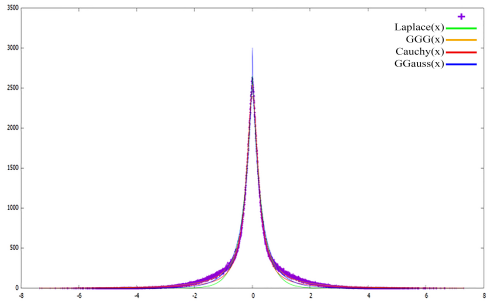

Figure A34. Histogram of 10^7 normalised Fourier coefficients of second Hecke eigenform of weight $49/2$ and distributions

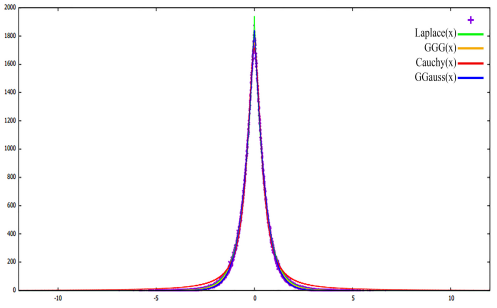

Figure A35. Histogram of 10^7 normalised Fourier coefficients of third Hecke eigenform of weight $49/2$ and distributions

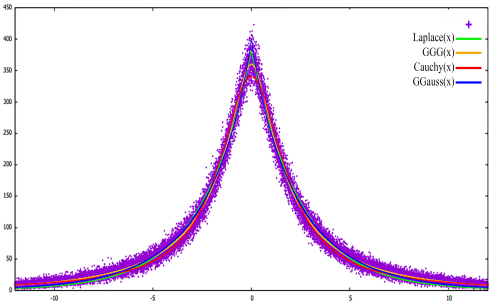

Figure A36. Histogram of 10^7 normalised Fourier coefficients of fourth Hecke eigenform of weight $49/2$ and distributions

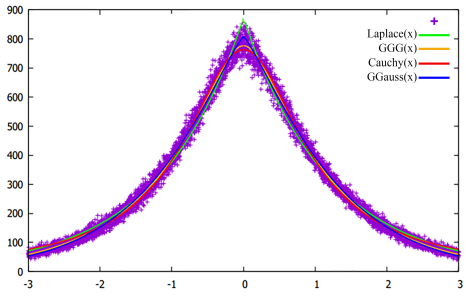

Figure A37. Histogram of 10^7 normalised Fourier coefficients of first Hecke eigenform of weight $51/2$ and distributions

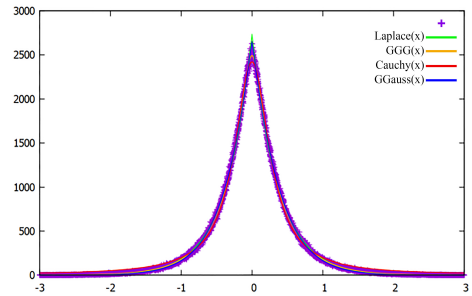

Figure A38. Histogram of 10^7 normalised Fourier coefficients of second Hecke eigenform of weight $51/2$ and distributions

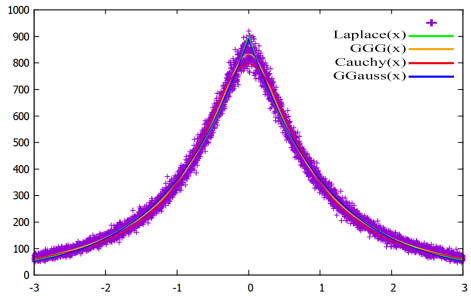

Figure A39. Histogram of 10^7 normalised Fourier coefficients of third Hecke eigenform of weight $51/2$ and distributions

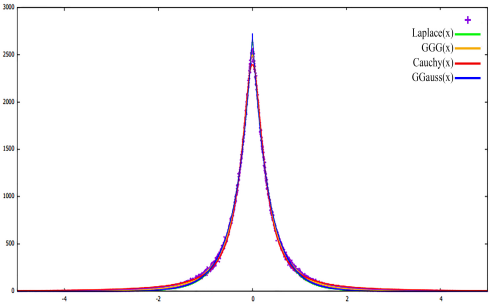

Figure A40. Histogram of 10^7 normalised Fourier coefficients of first Hecke eigenform of weight $53/2$ and distributions

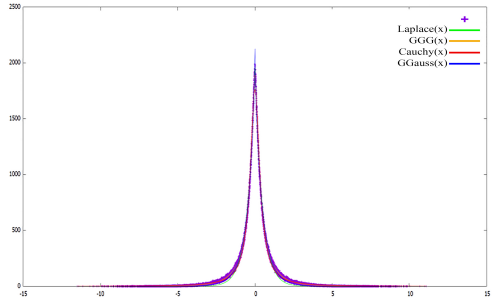

Figure A41. Histogram of 10^7 normalised Fourier coefficients of second Hecke eigenform of weight $53/2$ and distributions

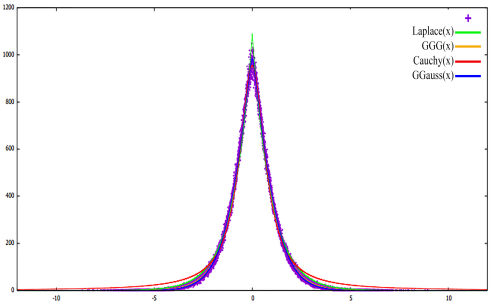

Figure A42. Histogram of 10^7 normalised Fourier coefficients of third Hecke eigenform of weight $53/2$ and distributions

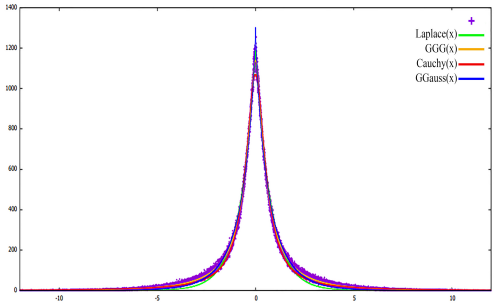

Figure A43. Histogram of 10^7 normalised Fourier coefficients of fourth Hecke eigenform of weight $53/2$ and distributions

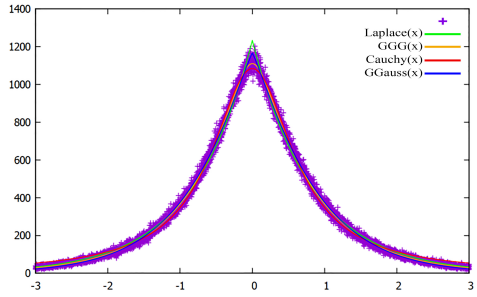

Figure A44. Histogram of 10^7 normalised Fourier coefficients of first Hecke eigenform of weight $55/2$ and distributions

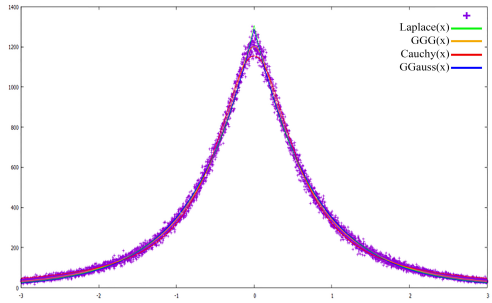

Figure A45. Histogram of 10^7 normalised Fourier coefficients of second Hecke eigenform of weight $55/2$ and distributions

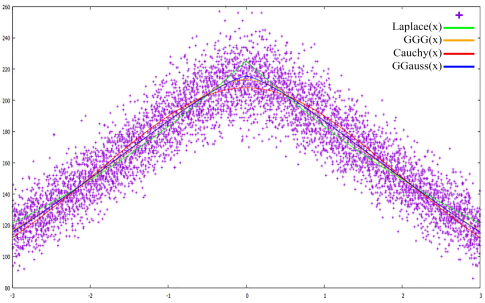

Figure A46. Histogram of 10^7 normalised Fourier coefficients of third Hecke eigenform of weight $55/2$ and distributions

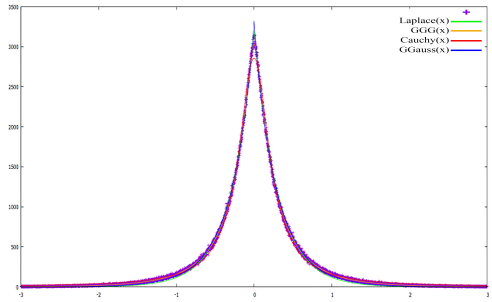

Figure A47. Histogram of 10^7 normalised Fourier coefficients of fourth Hecke eigenform of weight $55/2$ and distributions

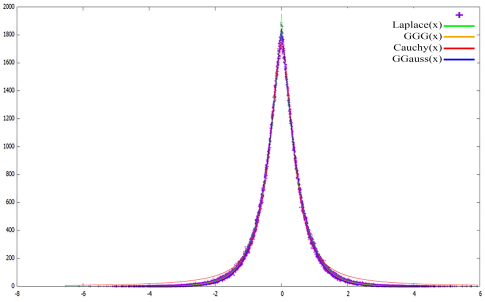

Figure A48. Histogram of 10^7 normalised Fourier coefficients of first Hecke eigenform of weight $57/2$ and distributions

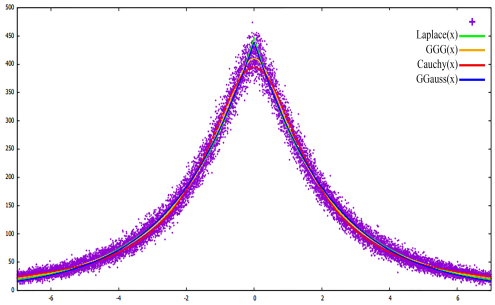

Figure A49. Histogram of 10^7 normalised Fourier coefficients of second Hecke eigenform of weight $57/2$ and distributions

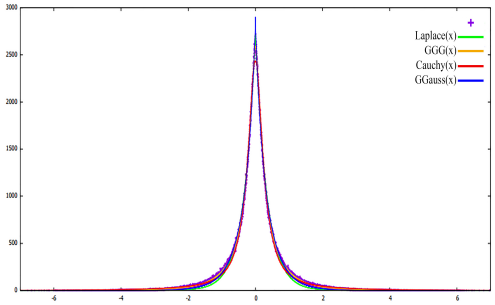

Figure A50. Histogram of 10^7 normalised Fourier coefficients of third Hecke eigenform of weight $57/2$ and distributions

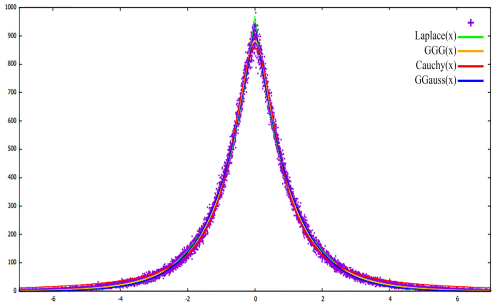

Figure A51. Histogram of 10^7 normalised Fourier coefficients of fourth Hecke eigenform of weight $57/2$ and distributions

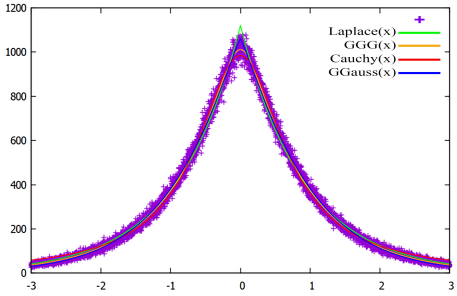

Figure A52. Histogram of 10^7 normalised Fourier coefficients of first Hecke eigenform of weight $59/2$ and distributions

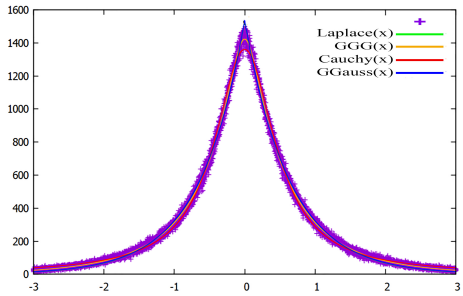

Figure A53. Histogram of 10^7 normalised Fourier coefficients of second Hecke eigenform of weight $59/2$ and distributions

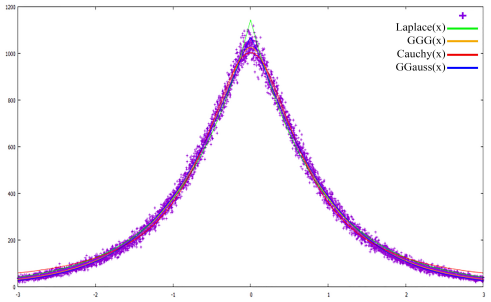

Figure A54. Histogram of 10^7 normalised Fourier coefficients of third Hecke eigenform of weight $59/2$ and distributions

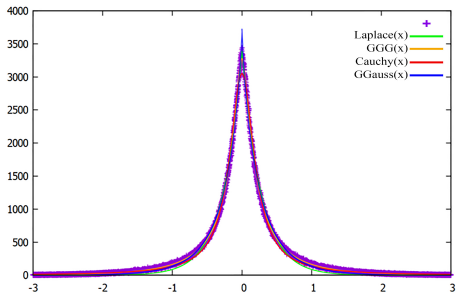

Figure A55. Histogram of 10^7 normalised Fourier coefficients of fourth Hecke eigenform of weight $59/2$ and distributions

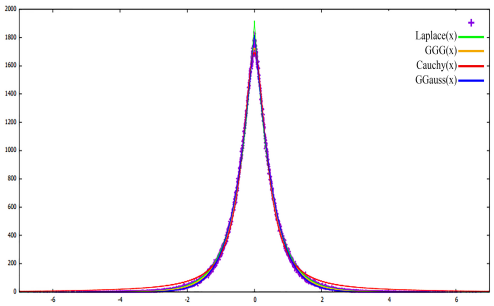

Figure A56. Histogram of 10^7 normalised Fourier coefficients of first Hecke eigenform of weight $61/2$ and distributions

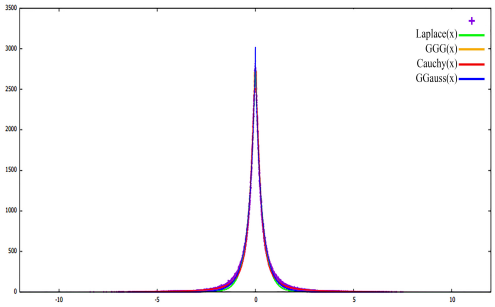

Figure A57. Histogram of 10^7 normalised Fourier coefficients of second Hecke eigenform of weight $61/2$ and distributions

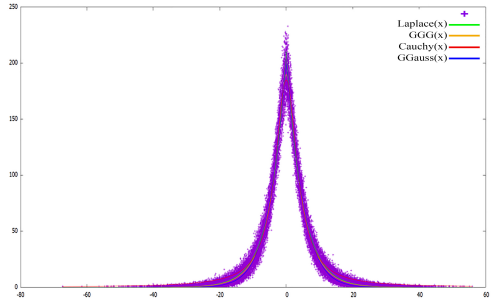

Figure A58. Histogram of 10^7 normalised Fourier coefficients of third Hecke eigenform of weight $61/2$ and distributions

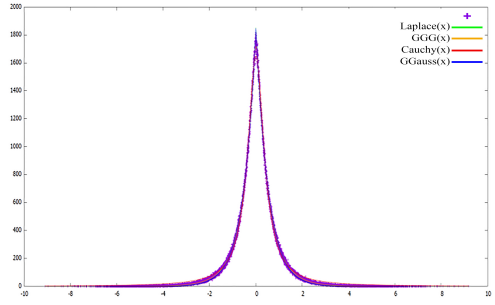

Figure A59. Histogram of 10^7 normalised Fourier coefficients of fourth Hecke eigenform of weight $61/2$ and distributions

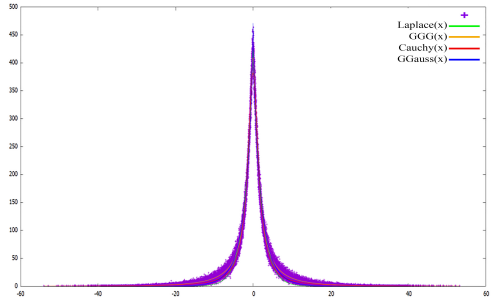

Figure A60. Histogram of 10^7 normalised Fourier coefficients of fifth Hecke eigenform of weight $61/2$ and distributions

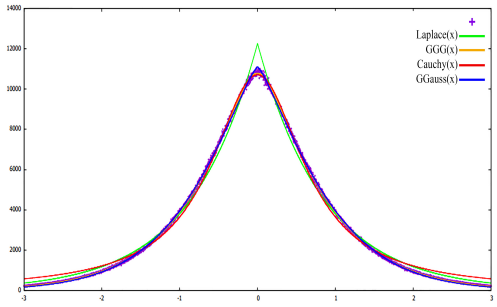

Figure A61. Histogram of 10^8 normalised Fourier coefficients of Hecke eigenform of weight 13/2 and distributions

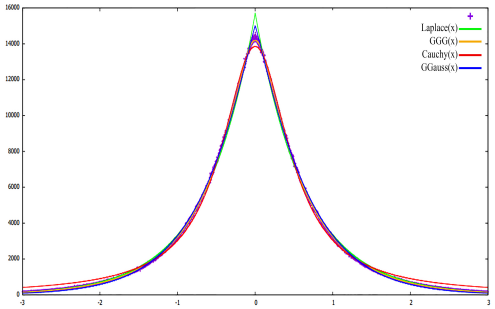

Figure A62. Histogram of 10^8 normalised Fourier coefficients of Hecke eigenform of weight 17/2 and distributions

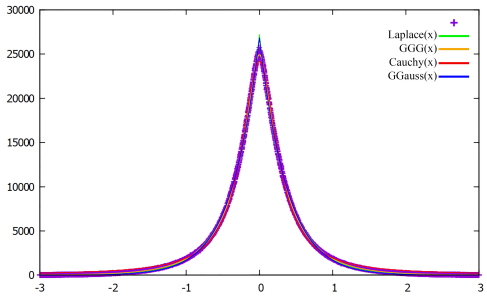

Figure A63. Histogram of 10^8 normalised Fourier coefficients of Hecke eigenform of weight 19/2 and distributions

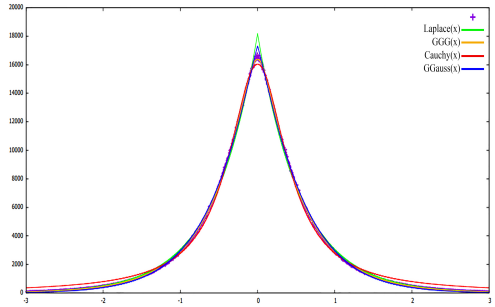

Figure A64. Histogram of 10^8 normalised Fourier coefficients of Hecke eigenform of weight 21/2 and distributions

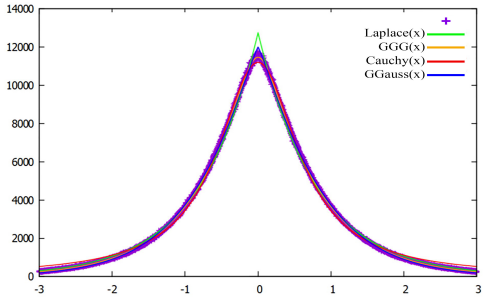

Figure A65. Histogram of 10^8 normalised Fourier coefficients of Hecke eigenform of weight 23/2 and distributions

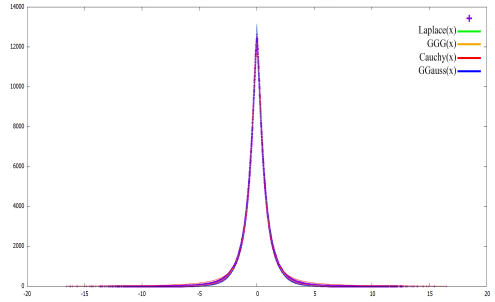

Figure A66. Histogram of 10^8 normalised Fourier coefficients of first Hecke eigenform of weight 25/2 and distributions

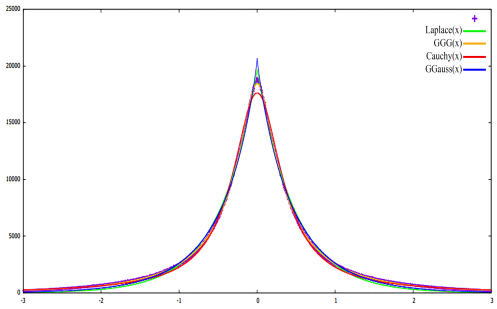

Figure A67. Histogram of 10^8 normalised Fourier coefficients of second Hecke eigenform of weight $25/2$ and distributions

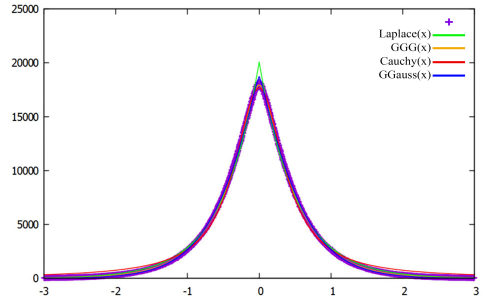

Figure A68. Histogram of 10^8 normalised Fourier coefficients of Hecke eigenform of weight $27/2$ and distributions

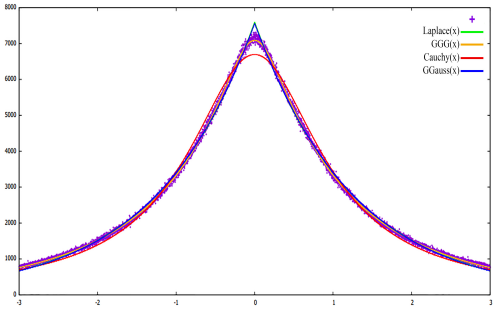

Figure A69. Histogram of 10^8 normalised Fourier coefficients of first Hecke eigenform of weight $29/2$ and distributions

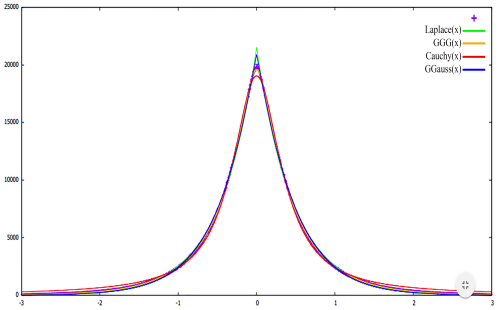

Figure A70. Histogram of 10^8 normalised Fourier coefficients of second Hecke eigenform of weight $29/2$ and distributions

Appendix: Graphs of histograms in weight 13/2 with $2 \cdot 10^8$ coefficients in 20 subsets

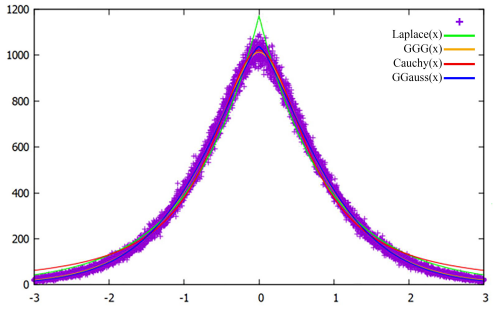

Figure A71. 1st part

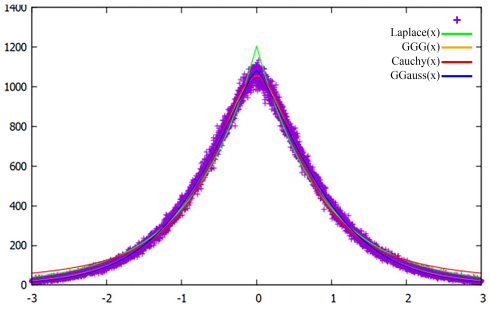

Figure A72. 2nd part

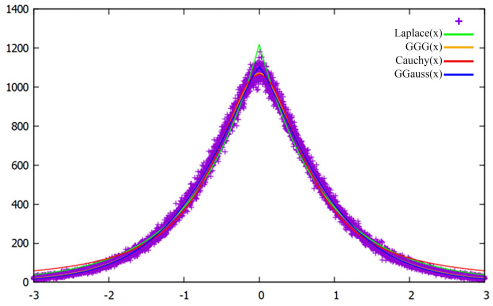

Figure A73. 3rd part

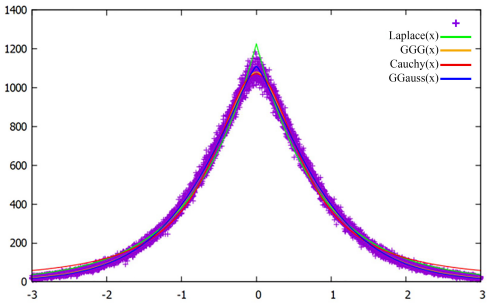

Figure A74. 4th part

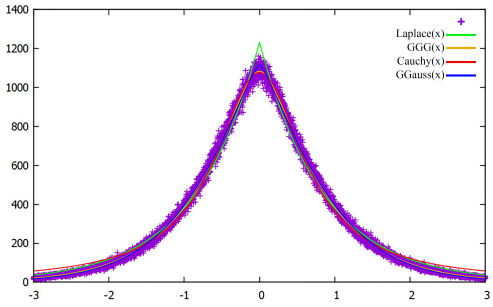

Figure A75. 5th part

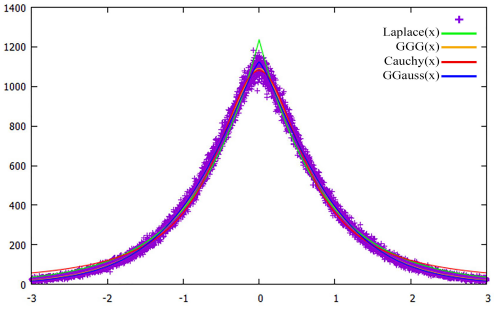

Figure A76. 6th part

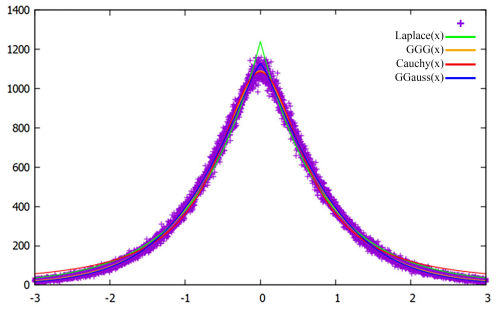

Figure A77. 7th part

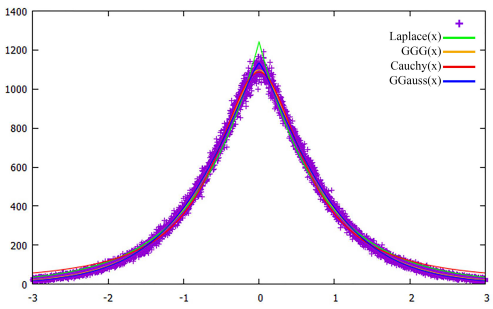

Figure A78. 8th part

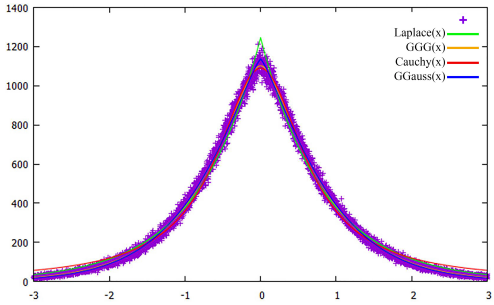

Figure A79. 9th part

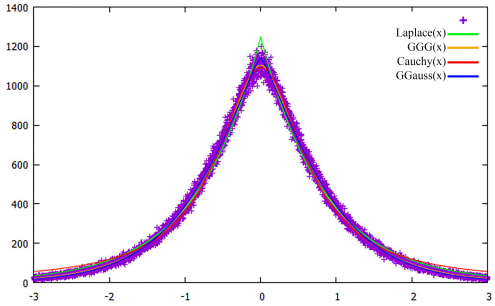

Figure A80. 10th part

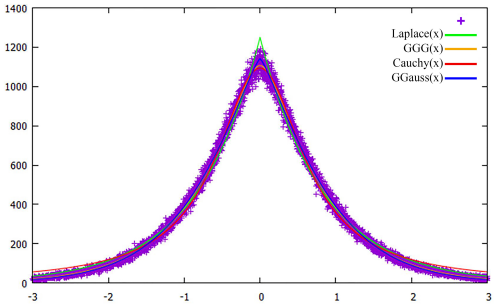

Figure A81. 11th part

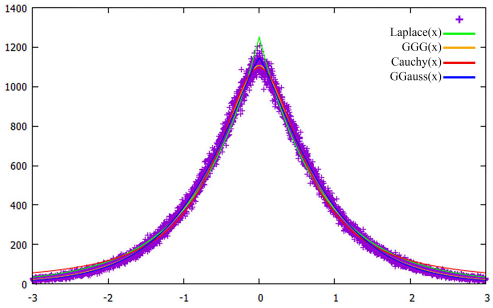

Figure A82. 12th part

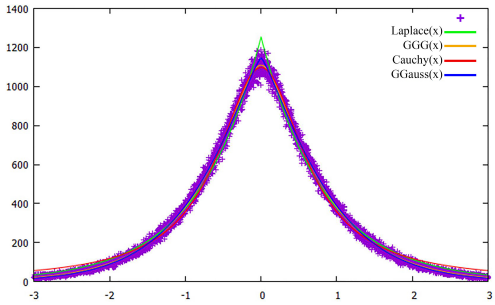

Figure A83. 13th part

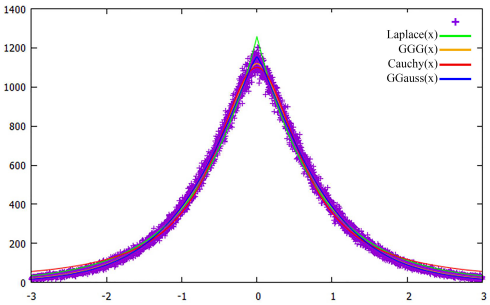

Figure A84. 14th part

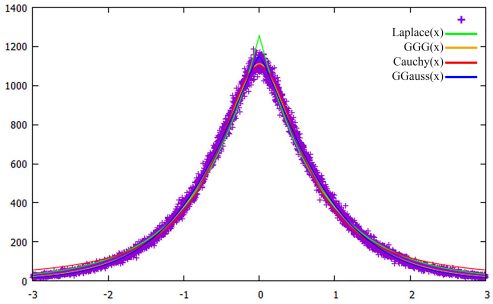

Figure A85. 15th part

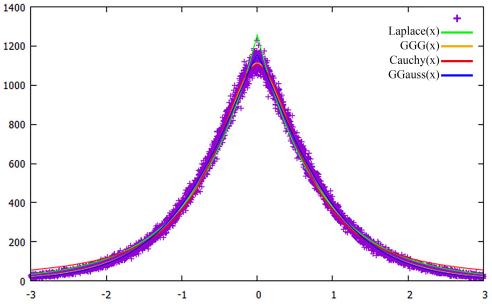

Figure A86. 16th part

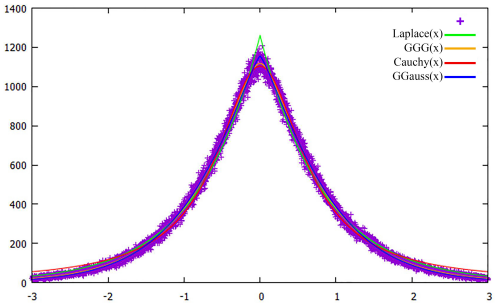

Figure A87. 17th part

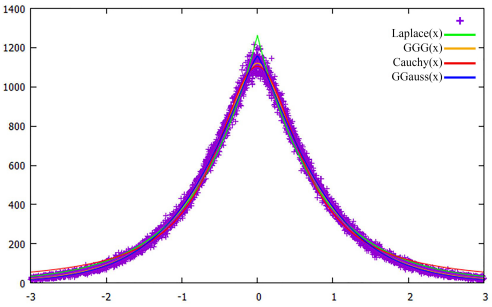

Figure A88. 18th part

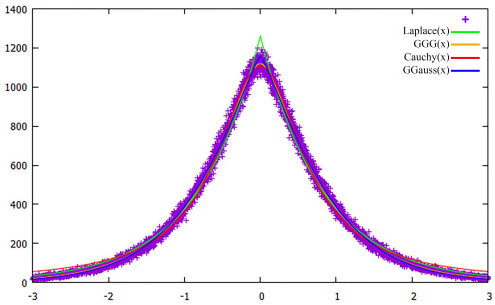

Figure A89. 19th part

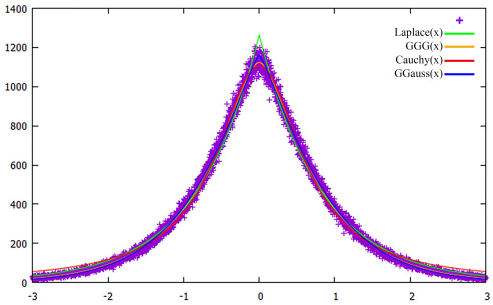

Figure A90. 20th part

Appendix: Tables of best fit parameters

Best fit parameters (rounded) for the GGG-distribution for all examples with 10^7 coefficients:

	a	b	c	d
13/2	0.622	1177.4	0.967	0.045
17/2	0.470	1986.6	0.575	0.043
19/2	0.386	4595.4	0.318	0.018
21/2	0.477	2268.8	0.506	0.032
23/2	0.527	1358.6	0.800	0.039
25/2(1)	0.384	2065.3	0.570	0.057
25/2(2)	0.219	12428.5	0.262	0.048
27/2	0.542	2129.2	0.498	0.018
29/2	0.354	1272.2	0.789	0.147
31/2(1)	0.468	2404.4	0.469	0.019
31/2(2)	0.375	2162.2	0.555	0.061
33/2(1)	0.508	1510.6	0.721	0.038
33/2(2)	0.338	4206.6	0.3526	0.017
35/2(1)	0.185	30546.8	0.195	0.014
35/2(2)	0.595	61.6	30.3975	6.408
37/2(1)	0.248	7668.0	0.292	0.022
37/2(2)	0.384	3432.2	0.397	0.035
37/2(3)	0.414	620.5	1.507	0.415
39/2(1)	0.397	2286.9	0.519	0.035
39/2(2)	0.508	2217.3	0.493	0.021
41/2(1)	0.439	1830.7	0.609	0.037
41/2(2)	0.334	4608.3	0.329	0.012
41/2(3)	0.441	1534.6	0.708	0.048
43/2(1)	0.307	2131.8	0.552	0.080
43/2(2)	0.548	1252.9	0.879	0.043
43/2(3)	0.232	12488.3	0.238	0.011
45/2(1)	0.419	3505.8	0.357	0.012
45/2(2)	0.492	928.6	1.172	0.116
45/2(3)	0.299	3046.2	0.443	0.038
47/2(1)	0.408	2253.6	0.521	0.033
47/2(2)	0.403	929.1	1.049	0.147
47/2(3)	0.475	2714.2	0.412	0.013
49/2(1)	0.439	1428.2	0.760	0.064
49/2(2)	0.094	798896	0.121	0.022
49/2(3)	0.480	2317.8	0.474	0.015
49/2(4)	0.269	1124.0	0.782	0.648
51/2(1)	0.509	1026.3	1.075	0.094
51/2(2)	0.442	3572.5	0.335	0.008
51/2(3)	0.369	1488.4	0.713	0.091
53/2(1)	0.339	5188.6	0.306	0.012
53/2(2)	0.274	4932.5	0.341	0.017
53/2(3)	0.570	1143.5	0.979	0.0478
53/2(4)	0.220	5509.5	0.350	0.067
55/2(1)	0.475	1518.7	0.718	0.043
55/2(2)	0.392	1998.2	0.574	0.043
55/2(3)	0.567	235.1	5.046	0.286
55/2(4)	0.338	5684.9	0.280	0.006
57/2(1)	0.488	2320.4	0.473	0.016
57/2(2)	0.378	735.0	1.237	0.422
57/2(3)	0.276	7174.6	0.281	0.011
57/2(4)	0.415	1401.3	0.771	0.083
59/2(1)	0.479	1351.5	0.796	0.047
59/2(2)	0.365	2562.3	0.481	0.031
59/2(3)	0.515	1281.0	0.841	0.038
59/2(4)	0.249	10585.4	0.241	0.006
61/2(1)	0.465	2445.7	0.465	0.020
61/2(2)	0.283	6542.5	0.286	0.008
61/2(3)	0.450	285.4	3.280	1.910
61/2(4)	0.395	2718.4	0.445	0.018
61/2(5)	0.167	4656.1	0.375	0.580

Best fit parameters (rounded) for the GG-distribution for all examples with 10^7 coefficients:

	a	b	c
13/2	0.677	1038	1.08
17/2	0.581	1406	0.71
19/2	0.538	2513	0.37
21/2	0.585	1622	0.60
23/2	0.599	1128	0.93
25/2(1)	0.525	1232	0.80
25/2(2)	0.467	1946	0.51
27/2	0.615	1756	0.54
29/2	0.529	708	1.37
31/2(1)	0.560	1817	0.53
31/2(2)	0.523	1232	0.80
33/2(1)	0.590	1211	0.85
33/2(2)	0.481	2243	0.44
35/2(1)	0.428	3402	0.32
35/2(2)	0.646	57	43.86
37/2(1)	0.437	2291	0.45
37/2(2)	0.540	1862	0.52
37/2(3)	0.529	418	2.55
39/2(1)	0.518	1470	0.68
39/2(2)	0.593	1744	0.56
41/2(1)	0.540	1319	0.76
41/2(2)	0.471	2532	0.40
41/2(3)	0.539	1123	0.91
43/2(1)	0.458	1025	0.93
43/2(2)	0.614	1061	1.02
43/2(3)	0.426	3277	0.33
45/2(1)	0.528	2396	0.40
45/2(2)	0.579	724	1.55
45/2(3)	0.448	1444	0.67
47/2(1)	0.524	1499	0.66
47/2(2)	0.509	642	1.57
47/2(3)	0.562	2105	0.45
49/2(1)	0.542	1023	1.01
49/2(2)	0.390	3004	0.36
49/2(3)	0.561	1841	0.53
49/2(4)	0.453	400	2.14
51/2(1)	0.606	807	1.39
51/2(2)	0.537	2644	0.36
51/2(3)	0.519	889	1.10
53/2(1)	0.486	2725	0.37
53/2(2)	0.426	2126	0.48
53/2(3)	0.630	986	1.13
53/2(4)	0.417	1304	0.72
55/2(1)	0.568	1165	0.88
55/2(2)	0.516	1287	0.77
55/2(3)	0.670	216	7.00
55/2(4)	0.463	3322	0.31
57/2(1)	0.568	1844	0.53
57/2(2)	0.529	438	2.36
57/2(3)	0.438	2903	0.36
57/2(4)	0.530	943	1.08
59/2(1)	0.568	1060	0.98
59/2(2)	0.496	1539	0.64
59/2(3)	0.586	1068	0.99
59/2(4)	0.416	3728	0.30
61/2(1)	0.562	1818	0.54
61/2(2)	0.430	3023	0.35
61/2(3)	0.579	199	6.74
61/2(4)	0.502	1848	0.54
61/2(5)	0.406	472	1.61

Best fit parameters (rounded) for the Laplace distribution for all examples with 10^7 coefficients:

	b	c
13/2	1172	0.908
17/2	1503	0.683
19/2	2600	0.388
21/2	1740	0.592
23/2	1220	0.850
25/2(1)	1260	0.791
25/2(2)	1884	0.511
27/2	1923	0.542
29/2	725	1.317
31/2(1)	1914	0.533
31/2(2)	1258	0.789
33/2(1)	1302	0.793
33/2(2)	2202	0.444
35/2(1)	3147	0.295
35/2(2)	62	17.400
37/2(1)	2140	0.440
37/2(2)	1930	0.522
37/2(3)	429	2.341
39/2(1)	1495	0.669
39/2(2)	1881	0.550

	b	c
41/2(1)	1367	0.740
41/2(2)	2458	0.395
41/2(3)	1163	0.897
43/2(1)	981	0.980
43/2(2)	1160	0.899
43/2(3)	3021	0.309
45/2(1)	2461	0.409
45/2(2)	774	1.331
45/2(3)	1366	0.699
47/2(1)	1532	0.655
47/2(2)	647	1.539
47/2(3)	2219	0.460
49/2(1)	1063	0.953
49/2(2)	2650	0.333
49/2(3)	1940	0.527
49/2(4)	381	2.493
51/2(1)	871	1.196
51/2(2)	2734	0.370
51/2(3)	903	1.077
53/2(1)	2687	0.364

	b	c
53/2(2)	1958	0.479
53/2(3)	1090	0.962
53/2(4)	1188	0.778
55/2(1)	1233	0.830
55/2(2)	1306	0.760
55/2(3)	225	4.846
55/2(4)	3197	0.303
57/2(1)	1954	0.525
57/2(2)	448	2.206
57/2(3)	2716	0.349
57/2(4)	969	1.039
59/2(1)	1121	0.912
59/2(2)	1533	0.642
59/2(3)	1144	0.902
59/2(4)	3389	0.274
61/2(1)	1918	0.532
61/2(2)	2796	0.336
61/2(3)	211	4.830
61/2(4)	1852	0.536
61/2(5)	423	2.131

Best fit parameters (rounded) for the Cauchy distribution for all examples with 10^7 coefficients:

	a	b	c
13/2	143	0.14	0.49
17/2	154	0.12	0.61
19/2	152	0.07	0.82
21/2	150	0.10	0.64
23/2	156	0.15	0.54
25/2(1)	163	0.15	0.59
25/2(2)	169	0.10	0.78
27/2	148	0.09	0.66
29/2	162	0.25	0.46
31/2(1)	156	0.09	0.68
31/2(2)	163	0.15	0.59
33/2(1)	156	0.14	0.56
33/2(2)	163	0.08	0.81
35/2(1)	212	0.07	1.17
35/2(2)	422	7.75	0.19
37/2(1)	200	0.10	0.93
37/2(2)	156	0.09	0.71
37/2(3)	5310	13.99	1.96
39/2(1)	175	0.13	0.67
39/2(2)	145	0.09	0.66
41/2(1)	161	0.13	0.61
41/2(2)	196	0.09	0.95
41/2(3)	147	0.14	0.53
43/2(1)	192	0.22	0.60
43/2(2)	145	0.14	0.51
43/2(3)	243	0.09	1.23
45/2(1)	287	0.13	1.10
45/2(2)	153	0.24	0.44
45/2(3)	206	0.17	0.74
47/2(1)	164	0.12	0.66

	a	b	c
47/2(2)	165	0.29	0.43
47/2(3)	151	0.08	0.74
49/2(1)	163	0.17	0.54
49/2(2)	211	0.09	1.14
49/2(3)	152	0.09	0.70
49/2(4)	1070	3.14	-0.90
51/2(1)	13	0.02	0.13
51/2(2)	12	0.00	0.23
51/2(3)	952	1.20	1.23
53/2(1)	169	0.07	0.91
53/2(2)	219	0.12	0.94
53/2(3)	144	0.15	0.49
53/2(4)	216	0.20	0.73
55/2(1)	580	0.54	1.06
55/2(2)	1857	1.61	2.04
55/2(3)	1459	7.01	0.82
55/2(4)	3681	1.29	4.70
57/2(1)	149	0.59	0.69
57/2(2)	65049	164.83	7.08
57/2(3)	208	0.09	1.05
57/2(4)	163	0.19	0.52
59/2(1)	1383	1.41	1.57
59/2(2)	2525	1.86	2.62
59/2(3)	385	28.90	24.97
59/2(4)	88133	0.30	2.55
61/2(1)	151	0.09	0.69
61/2(2)	242	0.10	1.17
61/2(3)	3403	18.40	-1.07
61/2(4)	169	0.10	0.74
61/2(5)	1346	3.52	-1.12

RMS values (rounded) for all examples with 10^7 coefficients:

	GG	GGG	Laplace	Cauchy
13/2	19	18	39	33
17/2	21	18	29	28
19/2	27	19	30	34
21/2	21	18	31	33
23/2	19	18	28	26
25/2(1)	21	18	22	22
25/2(2)	33	19	35	25
27/2	19	17	37	41
29/2	18	16	18	20
31/2(1)	22	19	28	33
31/2(2)	21	17	22	21
33/2(1)	19	18	28	27
33/2(2)	27	18	28	30
35/2(1)	48	20	57	40
35/2(2)	5	5	5	5
37/2(1)	26	14	30	25
37/2(2)	20	15	22	25
37/2(3)	9	9	9	10
39/2(1)	16	12	16	20
39/2(2)	17	15	28	34
41/2(1)	14	12	16	20
41/2(2)	22	14	24	27
41/2(3)	13	11	14	18
43/2(1)	13	9	13	14
43/2(2)	14	13	22	25
43/2(3)	41	19	50	41
45/2(1)	21	16	23	31
45/2(2)	11	10	13	16
45/2(3)	15	11	17	17
47/2(1)	16	13	16	21

	GG	GGG	Laplace	Cauchy
47/2(2)	10	9	10	12
47/2(3)	19	16	25	34
49/2(1)	13	11	14	17
49/2(2)	59	24	72	49
49/2(3)	17	15	23	31
49/2(4)	10	10	10	10
51/2(1)	18	17	24	20
51/2(2)	23	18	27	38
51/2(3)	20	17	20	21
53/2(1)	25	16	25	28
53/2(2)	20	12	26	25
53/2(3)	13	13	23	26
53/2(4)	17	10	20	17
55/2(1)	19	17	24	23
55/2(2)	21	18	22	23
55/2(3)	12	12	13	13
55/2(4)	30	18	34	39
57/2(1)	18	16	24	32
57/2(2)	12	12	12	12
57/2(3)	27	15	33	31
57/2(4)	13	11	14	16
59/2(1)	19	18	24	22
59/2(2)	23	17	23	25
59/2(3)	19	18	26	24
59/2(4)	40	19	54	48
61/2(1)	17	15	23	29
61/2(2)	34	18	43	42
61/2(3)	9	9	9	9
61/2(4)	17	13	17	23
61/2(5)	11	9	13	12